Laboratory of General Pathology and Immunology, Department of Surgical and Morphological Sciences, School of Medicine
University of Insubria, Varese, Italy

The Human T cell lymphotropic virus 1 (HTLV-1): cellular and molecular characterization of the HTLV-1 oncogenic protein HBZ

Goutham Utham Raval

A thesis submitted to the University of Insubria for the degree of Doctor of Philosophy

Project supervisor: Prof. Roberto S. Accolla

PhD Program Coordinator: Prof. Antonio Toniolo

Academic year: 2014/ 2015

ABSTRACT

T cell leukemia virus type 1 (HTLV-1) is the etiological agent responsible of a severe form of hematologic malignancy designated Adult T cell Leukemia/Lymphoma or ATLL and of a neurological syndrome designated HTLV Associated Myelopathy/Tropical Spastic Paraparesis or HAM/TSP. Although the major documented viral oncogenic product of HTLV-1 is the Tax-1 protein, it has been recently demonstrated that also HBZ (HTLV-1 bZIP factor), a protein encoded by the minus strand of HTLV-1 genome, is involved in the pathogenesis of ATL. The full role played by HBZ in oncogenesis is still to be explored in detail mainly owing to the unavailability of tools to study this protein in naturally infected cells and in ATLL cells and its interaction with other crucial cellular proteins involved in the homeostasis of cell activation and proliferation. By the use of the first reported monoclonal antibody against HBZ generated in our laboratory we have carefully analyzed HBZ protein expression, sub-cellular localization as well as its interaction in vivo with endogenous cell factors in various HBZ-expressing cells, including in particular HTLV-1-infected cells and ATLL tumor cell lines. We also demonstrated the ability of this monoclonal antibody to detect HBZ in fresh PBMCs of HTLV-1 infected patients. The availability of this newly generated anti-HBZ mAb has allowed for the first time the quantization of HBZ at the single cell level in naturally infected cells and in neoplastic cells, a better definition of HBZ expression, localization and functional involvement in the biology of HTLV-1 infected cells. The findings described in this thesis may help to better understand the mechanisms through which viral oncogenes contribute to immortalization and neoplastic transformation of the infected cell host.

Dedicated to

Mom & Dad: ***Utham S Raval & Lalitha U Raval***

Relatives: ***Neetu Kanubhai Raval & Daksha Sanjay Raval***

Wife: ***Priya G Raval***

Kiddos: ***Twinkle, Eshaan & Niashi Raval***

ACKNOWLEDGEMENTS

Completion of this doctoral dissertation was possible with the support of my family and several people listed below. I would like to express my sincere gratitude to all of them. Among them, I would like to specially thank my advisor ***Prof. Roberto S Accolla*** for his continuous support during my Ph.D study and research; for his patience, motivation, enthusiasm, and immense knowledge. Besides my supervisor, I would like to thank ***Dr. Carlo Bidoia*** for supporting me during the initial stages of my thesis project.

Prof. Roberto Accolla (Supervisor)

Prof. Giovanna Tosi (Senior researcher)

Dr. Carlo Bidoia (Ex co-supervisor)

Dr. Greta Forlani (Senior post-doc)

Dr. Luisa Merello (Previous post-doc)

Dr. Alessandra Tedeschi (Lab Technician)

Dr. Lamidi Badarau (Previous Doctoral)

Dr. Letizia Lombardy (Previous Doctoral)

Dr. Rawan Abdallah (Previous Doctoral)

Ms. Farah Bou Nasser Eddine (Current PhD)

Mr. Marco Baratello (Current PhD)

Ms. Luisa Guidali & stabulario staff (Confocal microscope Facility)

I am also grateful to my previous (masters degree) supervisor ***Dr. Neil Crickmore*** and lecturer (bachelors degree) **Dr. Madhan Shankar** for the basics of biological life science bestowed upon me. I extend my sincere thanks to all those teachers during different stages in my life, who taught me something. Finally, I would like to thank all my friends and well wishers of all age.

Faith does not give you the answers; it just stops you asking the questions

-Frater Ravus

If science proves some belief of religion wrong, then religion will have to change

-Dalai lama

ABBREVIATIONS

HTLV-1	Human T cell lymphotropic virus 1
HBZ	HTLV-1 bZIP factor
mAb	Monoclonal antibody
PBMC	Peripheral blood mononuclear cells
ATL	Adult T cell leukemia
HAM/ TSP	HTLV Associated Myelopathy/Tropical Spastic Paraparesis
sHBZ	Spliced HBZ
usHBZ	Unspliced HBZ
NFkB	Nuclear factor kappa B
CTL	Cytotoxic T cell
PEG	Poly ethylene glycol
HAT	Hypoxanthine Aminopterin Thymidine
GST	Glutathione S transferase
BCA	Bicinchoninic acid assay

TABLE OF CONTENTS

1. INTRODUCTION

1.1 HTLV-1 virus

The human T-cell lymphotropic virus type 1 (HTLV-1) is the first described human retrovirus and belongs to the deltaviridae family, subfamily oncovirus type C. Retroviruses are RNA viruses that use an enzyme called reverse transcriptase to produce DNA from their RNA. The newly produced DNA is subsequently incorporated into the host's genome. After integration retroviral particles can be produced and spread from cell to cell. The virion is about 100 nm in diameter and spherical in shape (Verdonck K et al.; 2007). The icosahedral capsid contains the viral RNA, and is within the protein inner envelope. The outermost layer is the lipid layer which is of host origin and contains the viral trans-membrane and surface proteins (Figure 1).

HTLV-1 is an oncogenic retrovirus that infects more than 20 million people worldwide (1,3). So far seven different HTLV-1 genotype (HTLV-1 *a* to HTLV-1 *g*) have been recognized (Verdonck K et al.; 2007). Beside HTLV-1 the Deltaretrovirus family include HTLV-2, HTLV-3, and HTLV-4; the simian T-cell lymphotropic viruses (STLV-1, STLV-2, and STLV-3) and the bovine leukemia virus (Matsuoka M et al., 2007). HTLV-1 is thought to be an old virus which originated in Africa, following multiple cross-species transmission from simians to humans some 27,000 years ago (Van Dooren S et al., 2001). It continued to spread overland to Asia, by sea routes to the Far East and by slave trade to America. The infection is now endemic in sub-Saharan Africa, Caribbean, South America, Japan, Melanesia and Middle East (Verdonck K et al., 2007). A curious observation is that within the endemic areas, the virus clusters in certain ethnic groups (Cooper SA et al., 2009). The virus is transmitted by sexual contact, blood transfusion and vertically from mother to

child. Worldwide, the major mode is sexual and the most efficient mode of transmission is blood transfusion (Bhigjee AI et al., 2014).

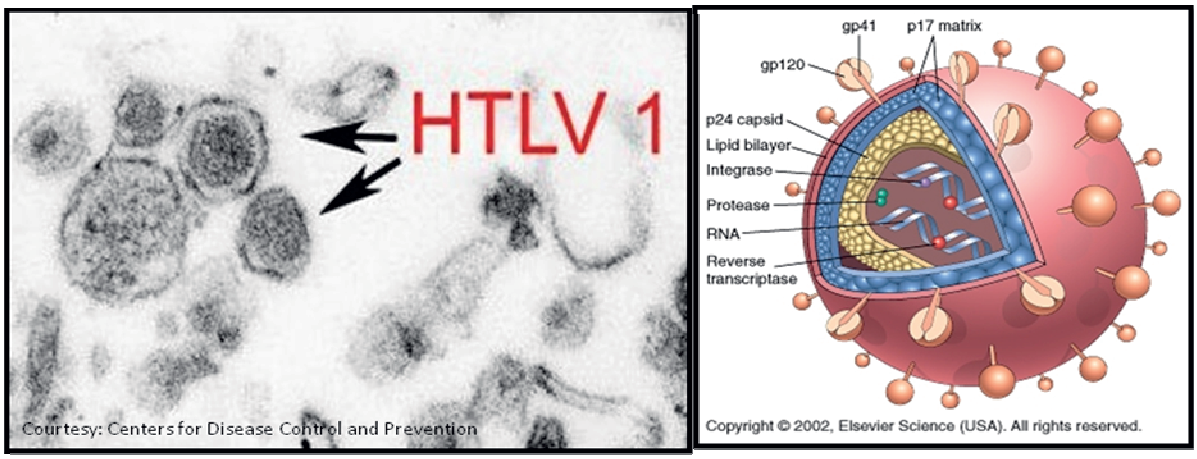

Figure 1: HTLV-1 virus as seen by electron microscope (left). Retrovirus structure (right)

1.2 Associated diseases

HTLV-1 was the first retrovirus associated with human diseases (Poiesz BJ *et al.,* 1980). HTLV-1 causes a fatal Adult T-cell leukemia/lymphoma (ATLL) that targets preferentially CD4+ T cells. The identification of HTLV-1 as the etiological agent of ATLL has allowed a detailed analysis of the epidemiological, immunological and clinical characteristics of this pathologic status (Takatsuki K et al., 1994). There are 4 clinical subtypes of ATL: smoldering, chronic, acute and lymphoma-type ATL (Satoshi T et al., 2004). Approximately 5% develop of HTLV-1 infected people develop ATL (Arisawa K et al., 2000) and another 2%-3% develop chronic inflammatory diseases involving the central nervous system (HTLV-associated Myelopathy/Tropical Spastic Paraparesis or HAM/TSP), the eyes (Mochizuki M et al., 1992), the lungs (Sugimoto M et al., 1987), the joints (Nishioka K et al., 1989), or the

skeletal muscles (Higuchi I et al., 1993); most infected individuals, however, remain healthy in their lifetime (healthy asymptomatic carriers: HCs).

Although the factors that cause these different manifestations of HTLV-1 infection are not fully understood, previous population studies suggested that both viral and host genetic factors influence the outcome of infection (Bangham CR et al., 2005). Moreover, although HTLV-1 primarily infects CD4+ T cells, other cell types in the peripheral blood of infected individuals have been found to contain HTLV-1, including CD8+ T cells, dendritic cells and B cells. HTLV-1 entry is mediated through interaction of the surface unit of the virion envelope glycoprotein (SU) with its cellular receptor *GLUT1*, a glucose transporter, on target cells (Manel N et al., 2003). HTLV-1.

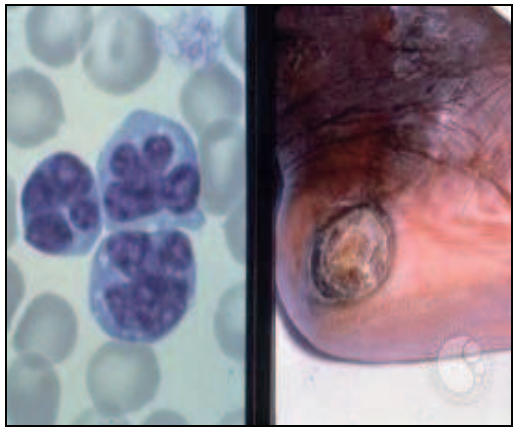

Fig 2: Adult-T cell leukemia flower cells (left) and ulceration (right).

Source: American Society of Hematology

1.3 HTLV-1 genome organization

The genome organization of all retroviruses is similar and includes *gag*, *pro*, *pol*, *env* genes (5' to 3'). The structural protein of the virion is encoded by *gag*, the viral protease is encoded by *pro*, reverse transcriptase enzyme is encoded by *pol* and the virion envelope glycoprotein

is encoded by *env* (Figure 3). Interestingly, HTLV-1 genome encodes for additional proteins that play a crucial role not only in the HTLV-1 genome expression but also in deregulation of host cell genome. The HTLV-1 genome expression is regulated by two regulatory genes, *rex* and *tax*, located in the 3' region of viral genome. Tax plays a key role in transactivation of viral transcription (Franklin A et al., 1995) (Thébault S et al., 2001). Rex plays a role in the transport of viral RNAs at the post-transcriptional level (Hidaka M et al., 1988). The other accessory genes encoded by the pX region are located between env and 3' LTR and include p30, p12, p21 and p13 (Franchini G et al., 2003). All these proteins are encoded by the plus-strand viral RNA.

Tax is certainly the best studied viral protein and is clearly implicated in the mechanisms leading to neoplastic transformation of the infected cells. Indeed Tax activates the nuclear factor k-B (NF-kB) pathway, cAMP response element-binding protein (CREB), activator protein-1 (AP-1) and serum responsive factor (SRF) (Yoshida M et al., 2001) from one side while inactivates p53 and by this inhibits apoptosis (Suzuki T et al., 1999). All these activities contribute to the uncontrolled proliferation of the cell (Franchini G et al., 2003).

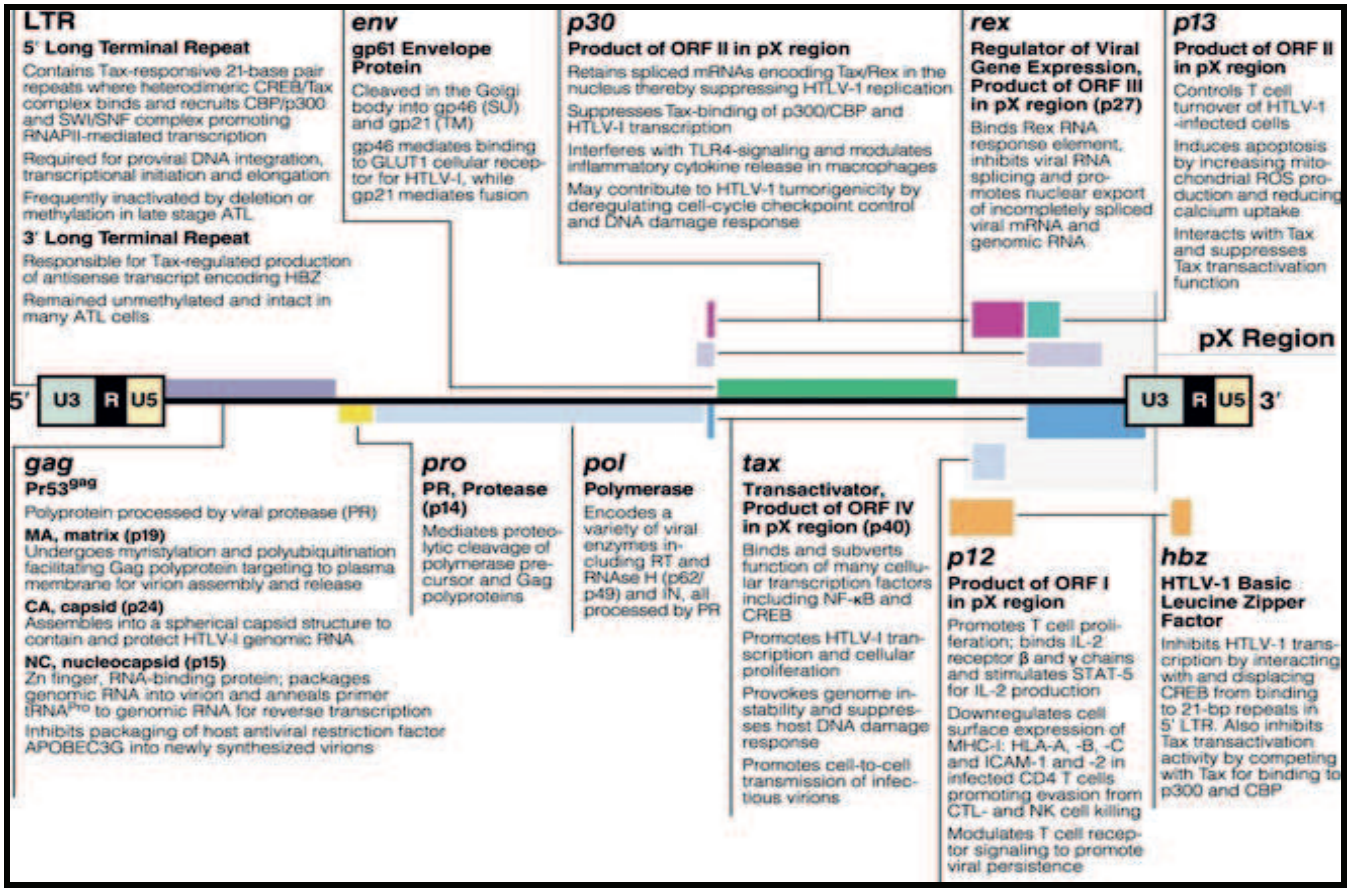

Fig 3: Genome organization of HTLV-1 provirus and functions of encoded proteins (Chan JK et al., 2012, Immunol Rev.)

1.4 The HTLV-1 bZIP factor, HBZ protein

The HTLV1 RNA genome also encodes a protein from the complementary strand (Gaudray G et al., 2002) designated HTLV-1 bZIP factor (*HBZ*). HBZ contains a bZIP domain in addition to an activation (N-terminus) and a central domain (Hivin P et al., 2005) (Figure 4). There are two different isoforms of this protein: a spliced form containing 206 amino acids (sp) and an unspliced form with 209 amino acids (us). The sp form is more abundant than the us form, is found in almost all ATL patients and its promoter is activated by the transcription factor SP1 (Yoshida M et al., 2008). Spliced HBZ is functionally stronger than unspliced HBZ in inhibiting transcription from viral 5´LTR. Promoters of spHBZ and usHBZ are

TATA-less and the transcription of spHBZ gene is relatively constant without Tax (Yoshida M et al., 2008). Indeed, HBZ was first identified as a protein interacting with CREB-2 via its bZIP domain and strongly inhibiting the CREB-2/Tax-1 interaction instrumental for the activation of HTLV-1 LTR (Gaudray G et al., 2002). Studies on the kinetics of HTLV-1 gene expression revealed nuclear retention of HBZ mRNAs (Rende F et al., 2011). Inhibition of T cell proliferation has been attributed to HBZ mRNA (Satou Y et al., 2006).

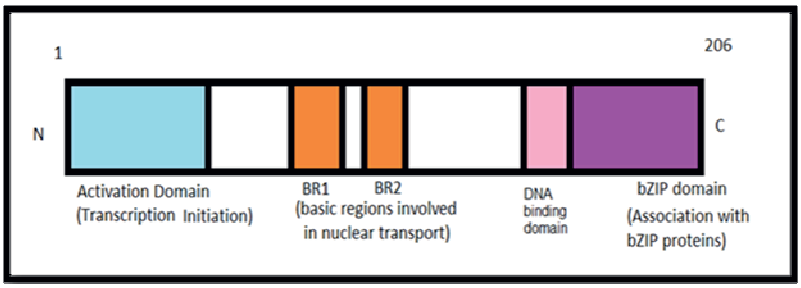

Domain	Function
AD	Bind with 26S proteasome Interact with CBP/p300 Activate TGF-β signaling
CD	Induce nuclear localization
bZIP	Interact and inhibit c-Jun, JunB, CREB, CREB2 Inhibit 5'LTR activation
AD+bZIP	Bind with p65, inhibit classical NF-kB pathway Ativate JunD Enhance hTERT promoter activity

Fig 4: Different domains of HBZ protein (top). Functions associated with different HBZ domains (bottom: modified from Zhao T et al., 2012, Frontiers in microbiology)

In addition to interacting with CREB-2, experiments using cells transfected with tagged HBZ have shown that HBZ binds to different proteins of the JUN family via its bZIP domain, experiments using cells transfected with tagged-HBZ have shown that HBZ binds to different proteins of the JUN family via its bZIP domain (Usui T et al., 2008). The binding to JunB

and cJun induces a sequestration of these factors in nuclear bodies or an accelerated degradation of them. As a result HBZ reduces the cJun/JunB-mediated transcriptional activation of a series of genes. Conversely, the binding of HBZ to JunD does not inhibit the JunD-mediated transcriptional activation of target genes; indeed HBZ-JunD complex upregulates even the expression of HBZ encoding gene (Basbous J et al., 2003; Mastumoto J wt al., 2005; Hivin P et al., 2007). Interestingly, in many cases HBZ exerts opposite effects with respect to Tax-1 on signaling pathways (Figures 5 and 6). HBZ interacts with the KIX domain of p300/CBP to disregulate their interaction with cellular factors and/or inhibit tax-dependent viral transactivation (Clerc I et al., 2008; Cook P R et al., 2011). HBZ inhibits, while Tax-1 activates, the classical NFkB pathway by inducing PDLIM2 expression which brings about proteasomal degradation of RelA (Zhao T et al., 2009). HBZ suppresses, while Tax-1 activates, Wnt pathway by interacting with the disheveled-associating protein with a high frequency of Leucine residues (DAPLE) (Ma G et al., 2012). HBZ inhibits production of Th1 cytokines (IFN-γ particularly) by interacting with NFAT and thus impairing cell-mediated immunity (Sugata K et al., 2012). Mice transgenic for HBZ showed an induced Foxp3 gene expression and subsequently an increase in the number of $CD4^{+}Foxp3^{+}$ T_{reg} cells, implicating its role in T cell lymphoma and inflammation in vivo (Satou Y et al.; 2011).

Conversely, HBZ enhances the effect of certain molecules and/or pathways. It activates telomerase by interacting with JunD and up-regulating the expression of hTERT (Kuhlmann A S et al., 2007); it enhances the TGF beta signaling pathway by interacting and forming a ternary complex with Smad3 and p300 (Zhao T et al., 2011).

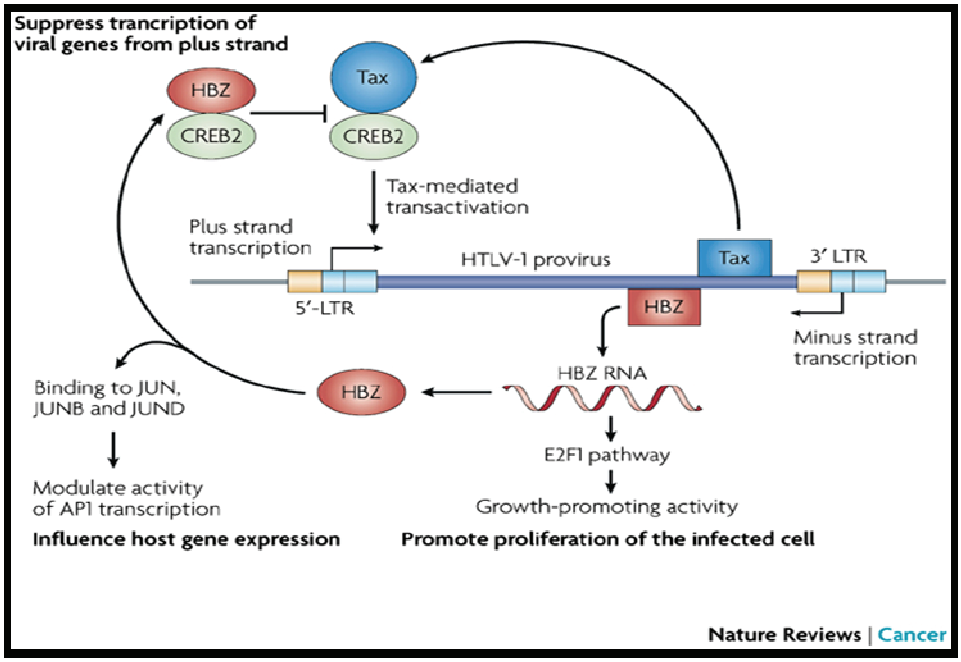

Fig 5: Mainstream HBZ activity (Matsuoka M et al., 2007)

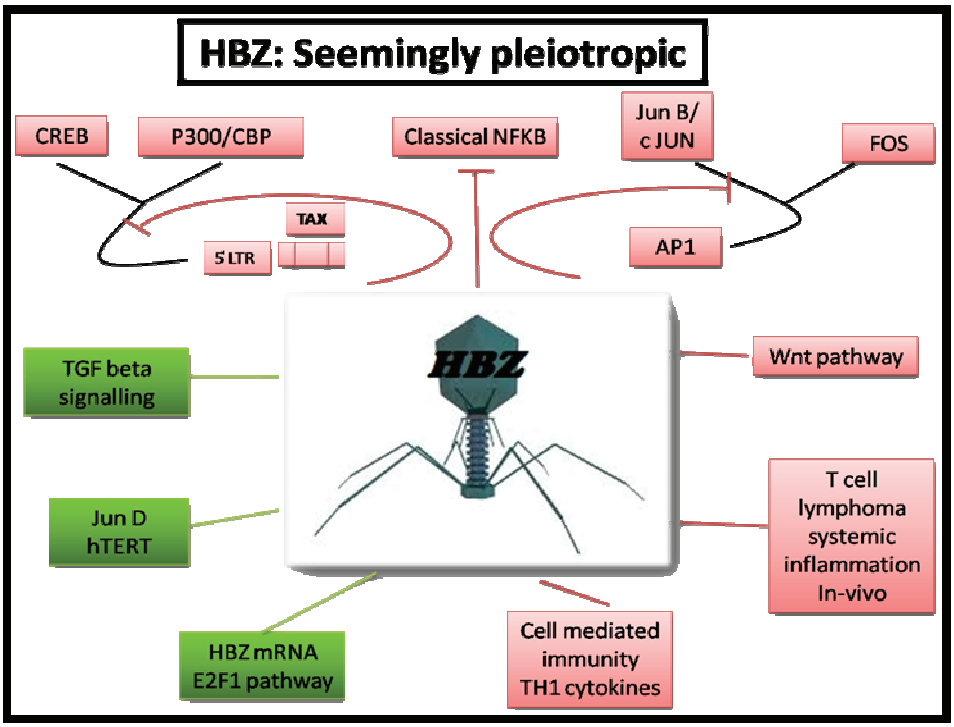

Fig 6: Pleiotropic effects of HBZ. Green and red represents pathways/ molecules activated and suppressed by HBZ respectively.

1.5 Mechanism of infection

HTLV-1 establishes a robust infection in CD4+ T lymphocytes (Kannian P et al., 2012). There is an increase in proviral load and Tax, Gag and Env (Fig. 7) during the initial stages of infection. This increase in viral proteins induces a humoral response and CTL activity in the host which eliminates most of the HTLV-1 infected cells (Macnamara A et al., 2010). HBZ might play a crucial role at this stage by down-regulating Tax-dependent viral transcription and rescuing the infected cells from host immune response (Barbeau B et al., 2013). Thus HBZ favors the establishment of persistent infection by conferring a survival advantage to HBZ-expressing cells (Arnold J et al., 2006). Although HBZ is not required for the immortalization of the infected cells, HBZ is important for proliferation of infected cells. Another observation clearly shows that HBZ transcript itself might be necessary for induced IL-2-independent T cell proliferation. (Satou Y et al., 2006).

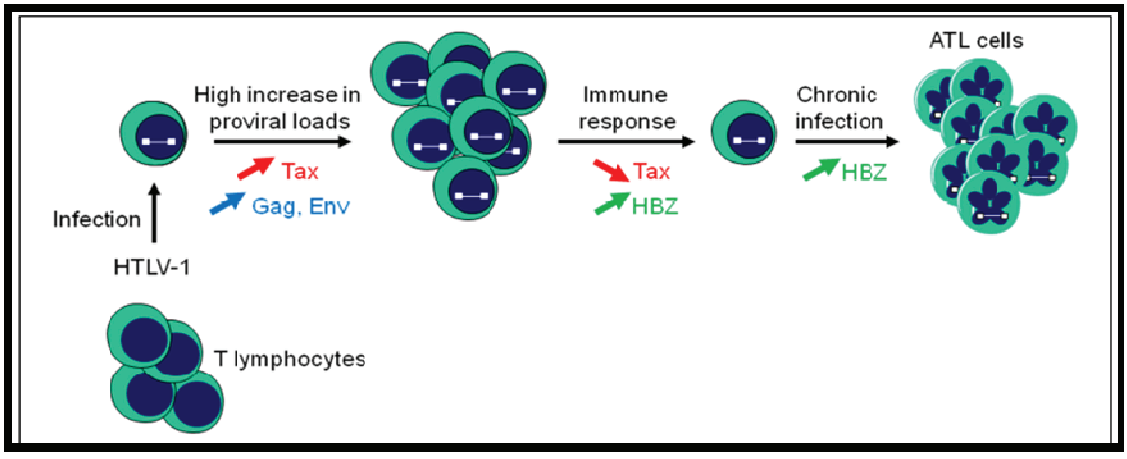

Fig 7: Proposed mechanism of HTLV-1 infection (Barbeau B et al., 2013).

2. AIMS OF THE STUDY

Most of the reported sub-cellular localizations, biochemical interactions with cellular components and consequent functional implications related to HBZ described above have been deduced by investigating cells transfected with HBZ in which the protein is usually overexpressed. The lack of suitable reagents such as monoclonal antibodies against the native, endogenous HBZ has not permitted to corroborate and validate all the functions attributed to HBZ, particularly in naturally HTLV-1 infected cells and in tumor cells of ATLL patients. The aim of this study was to fill-up this gap by generating a monoclonal antibody which can identify HBZ both in HBZ-transfected cells and, most importantly, in HTLV-1 infected and in ATLL tumor cells. This has allowed a more precise assessment of the subcellular localization of HBZ as well as its quantification *in vivo* both in HTLV-1 infected and in ATLL tumor cells and launched the premises for a better delineation of the role and presence of HBZ during HTLV-1 infection and cellular transformation.

3. MATERIALS AND METHODS

3.1 HBZ constructs

The recombinant HBZ plasmid pGEX2T-HBZ, used to prepare the recombinant GST-HBZ protein used for immunization (see below), was a gift of Dr. Lemasson, Univ East Carolina, USA (Clerc I et al., 2008). The myc-tagged and Hist-tagged HBZ were a gift of Dr. Matsuoka, Univ. of Kyoto, Japan (Satou Y et al., 2006). Full length and mutant fragments of GFP-tagged HBZ were provided by Dr. Mesnard, Montpellier, France (Hivin P et al., 2007).

To purify the recombinant protein (GST-HBZ), we used Pierce agarose glutathione beads (Thermo scientific, Rockford, USA). The beads were mixed with the supernatant of the bacterial lysate and incubated overnight on a rotor wheel at 4°C. Next day the beads were washed and the recombinant protein was eluted with elution buffer (Tris 50mM, Nacl 150mM pH 8, reduced glutathione 10mM).

3.2 Cells

COS and 293T cell lines were cultured in DMEM medium, supplemented with 10% fetal calf serum (FCS) and glutamine. HTLV-1 chronically infected cell line C5MJ (Balestrieri E, 2008) was kindly obtained from Dr. Macchi, University of Rome Tor Vergata and maintained in RPMI-FCS 10% . The ATL tumor cell line ATL-2s was obtained from Dr. Matsuoka, Japan (Takeda S et al., 2004). Peripheral blood monuclear cells (PBMC) PH961 were from an ATL patient, under the epidemiological control of the Pasteur Institute, Paris, France. The

immunophenotype of C5MJ, ATL-2s and patient PH961 PBMC was assessed by immunofluorescence and flow cytometry (BD FACSAria II™ apparatus) as described (Pellegrini FP et al., 2012) using monoclonal antibodies specific for HLA class I, HLA class II DR, CD3, CD4, CD8, CD25, CD19, CD16, CD127.

3.3 Mice immunization and generation of mAbs against HBZ

Immunization procedure and generation of monoclonal antibodies were essentially as described (Accolla RS et al., 1980). Six-week-old female BALB/c mice were injected intraperitoneally on day1 and day20 with 250 µl of a solution containing 10 µg of HBZ-GST protein with equal volume of Freund's Complete Adjuvant . On days 43 and 68, injections were repeated with Freund's Incomplete Adjuvant. Mouse serum was checked for anti-HBZ positivity before sacrificing on day 72. Total splenocytes were fused with 10 million P3U1 myeloma cells in presence of PEG as described (Accolla RS et al., 1980). The hybridomas were grown in RPMI complete medium with HAT (Hypoxanthine Aminopterin Thymidine) selection. Initial screening of hybridoma supernatants was performed by an indirect enzyme linked immunosorbent assay (protein detector ELISA kit, KPL). Briefly, 100µl of purified GST-HBZ protein (diluted in coating solution at 1µg/ml) was adsorbed onto the plate for 1h at RT. The plate was then blocked with 1x blocking solution for 1h at RT. The supernatant of the hybridoma to be tested was then added and incubated for 1h at RT. Peroxidase-labeled goat anti-mouse IgG was used as a secondary antibody. Finally the substrate and stop solution were added successively and the plate was read at 405 nm with a spectrophotometer. The mouse serum from immunized animals was used as a positive control and the supernatant of myeloma cells P3U1 or normal mouse serum served as a negative control. Hybridoma supernatants were screened for anti-HBZ positivity by western blot as well. To this purpose

cell lysates from Cos cells transfected with myc-tagged HBZ (see below) was run on a 10% SDS-PAGE gel and transferred onto nitrocellulose membrane (Amersham high bond ECL, GE, buckinghamshire, UK). The membrane was then quenched in 5% non fat milk in 1X TBS containing 0.05% Tween-20 (MTTBS) for 1h at room temperature. Hybridoma supernatant was diluted 1:1 with 5% MTTBS and used as primary antibody at 4°C O.N. After appropriate washes with MTTBS, HRP conjugated goat anti-mouse IgG was used as secondary antibody for 1h at room temperature. The membranes were developed by ECL system (Pierce, Rockford, USA) and exposed to X-ray film. A similar protocol was used for analyzing HBZ mutants and C5MJ/ ATL-2s lysate

To determine the antibody isotype, we used Pierce rapid ELISA mouse mAb isotyping kit. Appropriately diluted hybridoma supernatant was added to the wells pre-coated with anti-mouse heavy or anti-mouse light chain capture antibody. Goat anti-mouse IgG+IgM+IgA HRP conjugate was then added to the wells and incubated for 1 hr at room temperature. Following washes; TMB substrate and stop solution were added following manufacturer' instructions and finally the color developed was read at 450 nm.

3.4 Transfection procedures

COS cells or 293T cells were transfected with full length HBZ constructs (GFP-HBZ or myc-HBZ) or GFP-tagged HBZ fragments (ΔZIP, ΔAD, BR1, DBD, BR1-BR2-DBD) as previously described (Tosi G et al, 2011). COS and 293T cells were seeded in 35-mm-diameter plates and transfected with 1-3 μg of plasmid DNA constructs using Lipofectamine (Invitrogen). Cell extracts were prepared 24 h posttransfection and analyzed for the expression of recombinant proteins by SDS-PAGE and Western blotting with the following

antibodies: anti-Myc (9E10; Santa Cruz Biotechnology) to detect myc-tagged HBZ and anti-turboGFP (Origene) to detect GFP-tagged full length or fragment HBZs. Horseradish peroxidase (HRP)-conjugated anti-mouse immunoglobulin or anti-rabbit immunoglobulin secondary antibodies (Amersham) were used. Blots were developed by chemiluminescence assay (Immune-Star HRP substrate; Bio-Rad).

3.5 Quantitative assessment of HBZ in chronically infected and in ATLL tumor cell lines

Endogenous HBZ expression was quantitated by using the anti-HBZ monoclonal antibody 4D4-F3. To this purpose a standard curve with increasing concentrations of purified GST-HBZ protein was constructed and visualized by western blot with the anti-HBZ mAb. Cell lysates from both endogenously HBZ-producing cells and HBZ transfected cells were then assayed for the presence of HBZ by western blot and relative intensities compared by densitometry with those obtained in the standard curve. The deduced concentration of HBZ in cells was obtained by taking into account the total number of cells used for preparing the cell lysate, the volume of cell lysate used and the percentage of positive cells visualized by confocal microscopy. The obtained number in amount/cell was then converted in number of moles/cell taking into account the molecular weight of endogenous HBZ (assumed as 26.000 dalton), and transfected myc-tagged HBZ (myc-HBZ, 36.000 dalton) by the formula: [HBZ_{gr} / HBZ_{mw} = HBZ_{moles}]. Mole value (HBZ_{moles}) was then transformed in number of molecules/cell by multiplying it for the Avogadro number following the formula: $N_{molecules} = 6 \times 10^{23} \times HBZ_{moles}$.

3.6 Antibodies used for Immunophenotyping

the following monoclonal antibodies: mouse anti-human HLA class I (clone B9.12); mouse anti-human HLA class II DR (clone D1.12); mouse anti-human CD19 (clone HIB19, BD Pharmingen); mouse anti-human CD16 (clone3G8, BD Pharmingen, Milan, Italy); the above antibodies were revealed by FITC-labelled rabbit anti-mouse IgG F(ab')2 antiserum (Sigma, Milan, Italy); FITC mouse anti-human CD3 (clone (UCHT1 BD Pharmingen); FITC mouse anti-human CD4 (clone RPA-T4, BD Pharmingen); phycoerythrin (PE) mouse anti-human CD25 (clone M-A251, BD Pharmingen), PE-Cy5 mouse anti-human CD8a (clone RPA-T8; eBioscience, Milan, Italy) and AlexaFluor® 647 mouse anti-human CD127 (clone HIL-7R-M21, BD Pharmingen). Incubation and staining procedures were as previously described (Pellegrini FP et al., 2012).

3.7 Confocal microscopy

Appropriate number of cells were plated onto a sterilized cover slip (pre-coated with D-polylysine 0.1ug/ml, Sigma) placed in a six-well plate. After 24h, transfection with plasmid coding for myc-HBZ or GFP-HBZ or different HBZ mutants was performed overnight as desired. The cells were then washed with PBS 1X three times and fixed with methanol (-20°C) for 4-6 minutes. Cells were then washed three times with PBS, and incubated with a solution of 0.5 % BSA in PBS for 1 h. The anti-HBZ was then added as primary antibody and incubated overnight at 4°C. Alexa fluor 546 IgG1 goat anti-mouse was used as secondary antibody for detecting the monoclonal antibody. After three washes with PBS, finally the cover slip was mounted onto a glass slide using a drop of mounting medium and sealed. The

images were visualized by a Leica confocal microscope. A similar protocol was used for HTLV-1 infected cells C5MJ and ATL-2s. For the infected cells, PBS was replaced by a PHEM (60mM pipes, 25mM Hepes, 10mM EGTA, 2mM mgcl2; pH 7.0) buffer to improve the signal and the fixation was done by using absolute ethanol (-20°C) for 4-6 minutes. To assess co-localization of HBZ with host cellular factors C5MJ, ATL-2s and PH961 cells were reacted in a pairwise combination with the 4D4-F3 anti HBZ mAb antibody, and either polyclonal rabbit anti-CBP, anti-JunD, anti-p300, anti-CREB2, or anti-nucleolin. Anti-HBZ mAb was revealed by Alexa fluor 546-labeled goat anti-mouse IgG (red), whereas the other rabbit antibodies were revealed by Alexa fluor 488-labeled goat anti-rabbit antibodies (green).

3.8 Co-immunoprecipitation

Cell lysate of ATL-2s, C5MJ, PH961 cells as well as cell lysates of 293T cells transfected with a vector coding for HBZ.myc were prepared by using a non-denaturing lysis buffer (NP-40 1%, Tris-base 10mM Ph 7.4, Nacl 150mM, EDTA 2mM). Protein A sepharose beads (GE) were washed with the same lysis buffer and used for pre-clearing the lysate for 20 minutes at 4^0C. A volume of 100µ of anti-HBZ supernatant was then added to the precleared lysate and incubated for 1 h at 4^0C. Protein A sepharose beads were washed with lysis buffer and added to the above lysate; followed by overnight incubation at 4^0C. The beads were then washed six times with the same buffer (one time in between with lysis buffer containing high salt 500mM NACL). Finally the beads were resuspended in 50µl of loading buffer 2X, boiled and run on SDS gel. The membranes were then incubated with appropriate primary and secondary antibodies, exposed and developed.

3.9 Anti-HBZ ascites generation

To obtain high concentration of monoclonal antibody, 4D4-F3 hybridoma cells were injected intraperitoneally in Balb/c mice pre-injected 1 week before with 0,4 ml of pristane (Sigma) Ascitic fluid was collected after 2-3 weeks aseptically by using a syringe needle tip (22G). The resulting fluid was centrifuged to collect the supernatant. Aliquotes were made and freezed at -80 degree celcius until use.

3.10 cDNA synthesis and QRT-PCR

Total RNA was extracted from 5 million cells using Trizol (Invitrogen, Carlsbad, USA) and cDNA synthesized from total mRNA by using Iscript (Bio-Rad) according to the manufacturer's protocol. PCR was performed by using 1ul of RT reaction, Sybrgreen master mix (Life Technologies) and 10 uM each forward and reverse primers. The following primers were used for amplifying HBZ and hRPS7 transcripts: 5'-seq-3' (ATGGCGGCCTCAGGGCTGT), 5'-seq-3' (TGGAGGGCCCCGTCGCAG) and 5'-seq-3' (TGGAGATGAACTCGGACCTC), 5'-seq-3' (CGACCACCACCAACTTCAA) respectively. Q-RT-PCR was performed in an ABI Prism 7000 sequence detection system (Applied Biosystems) according to the manufacturer's instruction. The house-keeping human ribosomal protein S7 (hRPS7) was used as a reference control in the PCR reaction. The Ct value for each gene was obtained and was used to calculate the delta Ct value for each cell type, by the formula ΔCT = CT of target gene – CT of reference gene. The ΔΔCT value was then calculated for each cell type by the formula, ΔΔCT = ΔCT of cell type – ΔCT of standard. For our experiments the ΔCT value of C5MJ was kept as standard. Finally, the relative expression value was calculated by the formula 2^- ΔΔCT for each cell type.

4. RESULTS

4.1 HBZ.GST: production, purification and quantification

In order to generate monoclonal antibody against HBZ, GST-tagged HBZ fusion protein was used as an immunizing antigen. HBZ.GST protein was expressed in a bacterial source as explained in materials and methods. The bacterial cell lysate was subjected to a GST pull down assay in order to purify the expressed fusion protein (Fig. 8). Elution 1 and elution 2 lanes (Fig. 8, lane 6 and 7,) contained the eluted material coming from beads washed with reduced glutathione. The eluted material (HBZ.GST fusion protein) was by using a BCA protein assay kit and constructing a standard curve with know concentration of bovine serum albumin (BSA) (Fig. 9 and Fig. 10). The equation corresponding to R value of standard curve was used to calculate the unknown protein concentration. Substituting an absorbance value of 1.199 for HBZ.GST (elution 1) in the equation generated, a protein concentration value of 54.55 ng per ul was found (Fig. 10).

4.2 Anti-HBZ monoclonal antibody generation, screening, cloning and iso-typing

Mice was immunized with 10 ug of HBZ.GST purified protein. The immunization protocol was as described in materials and methods. Spleen cells of immunized mice were fused with myeloma cells (P3U1) using PEG (polyethylene glycol). The resulting hybridomas were selected in a HAT+ medium and screened by western blot (Fig. 11). In order to screen the fused hybridoma supernatant, myc-tagged HBZ fusion protein was expressed and verified by western blot (Fig 12). Out of 96 hybridomas screened, one designated 4D4 showed strong

positivity (Fig 13). The specificity for HBZ was demonstrated by the reactivity of the hybridoma with different tagged HBZ protein (HBZ.myc).

The original 4D4 hybridoma cells were cloned by limiting dilution to isolate purified monoclonal populations of cells from the bulk hybridoma culture. Supernatants from single clones were screened by using ELISA as described in materials and methods. Two clones D1 and F3 showed high positivity for anti-HBZ reactivity and two other B10 and C10 showed slight positivity (Fig 14). In an attempt to verify the ELISA results above, only D1 and F3 monoclone reacted against HBZ when screened by western blot (Fig 15). Among the two monoclones, 4D4.F3 was selected to be used for all further experiments unless otherwise mentioned. The anti-HBZ clone 4D4-F3 was isotyped as IgG1 with kappa light chain by using an ELISA kit (Fig. 16).

4.3 The 4D4-F3 mAb recognizes an epitope in the BR1 region of HBZ protein

In order to delineate the HBZ epitope region recognized by 4D4-F3, an epitope mapping was carried out. For this purpose lysates of Cos cells transfected with either wild type GFP-HBZ or a series of GFP-HBZ constructs were analyzed by western blot. As shown in the Fig. 17, A left western blot, 4D4-F3 mAb recognized all fragments including the basic region 1 (BR1) of HBZ, and particularly the isolated diagnostic BR1 fragment but not the isolated DBD fragment. On the basis of the above results, the epitope was mapped to the region between amino acids 97 to 133 (Fig 17B) including the BR1 region. In order to confirm that the different HBZ mutant proteins were indeed present in the corresponding lysate, the anti-serum from the mouse immunized with HBZ-GST and whose spleen was used for cell fusion,

was checked for reactivity with the various HBZ protein fragments. Results presented in Fig. 17A, right panel, clearly show the reactivity of the antiserum with all fragments including the DBD fragment which is not recognized by the anti-HBZ F3 monoclonal antibody. Figure 17B summarizes the results of epitope mapping, listing all the different HBZ constructs used and their size.

4.4 Sub-cellular localization of HBZ and its constructs as assessed by the 4D4-F3 monoclonal antibody

4D4-F3 mAb was used to assess the localization and the distribution of HBZ in transfected cells. Previous studies using green fluorescence protein (GFP)-tagged HBZ or myc-tagged HBZ constructs transfected in Cos or 293T cells have documented a nuclear localization of HBZ in characteristic nuclear speckles (Gaudray. G et al., 2002). In our hands, GFP-HBZ transfected in 293T cells also showed a distinct nuclear speckled distribution (Fig 18) coming from GFP fluorescence. When the same cells were incubated with the 4D4-F3 mAb very intense stainig in the speckle-like nuclear structure was identified with a virtually complete overlap with the GFP-HBZ staining (Fig. 18, merge column). Interestingly, however, when GFP-HBZ deletion mutants were analyzed, a more refined and selective staining by the 4D4-F3 antibody was observed (Fig. 19). For example nuclear GFP-ΔZIP and GFP-ΔAD fragments often displayed, beside spleckle-like distribution, strong green fluorescence staining in nuclear aggregates that were not detected by the 4D4-F3 which instead specifically evidentiated only the speckle-like structrures (see corresponding panels in Fig. 19), strongly suggesting that those GFP-related aggregates are indeed an artifact due to the GFP and not a real signal due to ΔZIP and ΔAD localization. Virtual overlap in the staining

between GFP and 4D4-F3 antibody was instead found for the mostly cytoplasmic BR1 and the mostly nuclear BR1-BR2-DBD HBZ fragments (see corresponding panels in Fig. 19), although, again, staining with 4D4-F3 was more refined and precise particularly for those few nuclear speckles observed with the BR1 fragment. Importantly, the DBD fragment was only evidentiated by the green fluorescence associated to the GFP-DBD construct and not by the 4D4-F3 antibody, further confirming epitope mapping by western blot (Fig. 17).

4.5 Untagged exogenous HBZ detected by 4D4-F3

To assess whether the specificity of 4D4-F3 for HBZ was in any way affected by tagging the protein, an untagged HBZ contruct was synthesized and transfected in293T cells. Briefly, the vector backbone and HBZ insert for DNA ligation were restricted with XbaI and HIndIII (Fig. 20A). The ligation product upon restriction check by EcoR1 and BamH1 (Fig. 20B) was used for protein expression. The ability of 4D4.F3 anti-HBZ monoclonal antibody to detect untagged HBZ protein expressed by the newly generated DNA vector in transfected cells was confirmed by western blot and confocal microscopy (Fig. 21). Untagged HBZ protein migrates slightly above 25KDa (Fig. 21A) in contrast to myc-tagged HBZ protein which migrates at 36 KDa. Untagged HBZ conserved the characteristic speckle-like distribution in the nucleus observed also with the myc-tagged protein (Fig. 21B). These results confirm that the 4D4-F3 mAb can indeed recognize an epitope whose antigenicity is not affected by tagging the HBZ protein, and thus paved the way to use the mAb for detection analysis in endogenously synthesized HBZ in HTLV-1 naturally infected and in HTLV-1 dependent ATL tumor cells.

4.6 Visualization of endogenous HBZ protein in HTLV-1 infected and in ATL tumor cells by 4D4-F3 mAb

Having demonstrated the specificity of the 4D4-F3 mAb both biochemically and phenotypically in HBZ transfected cell lines, it was then investigated the crucial aspect of detection and cellular distribution of endogenously made HBZ in HTLV-1 infected cells and cell lines. To this purpose three distinct cell lines were used: fresh peripheral blood mononuclear cells (PBMC) from a patient (PH961) suffering of ATL and two distinct cell lines, the HTLV-1 chronically infected C5MJ cell line (Sankichi H et al., 2006) and the ATL-2s cell line (Maeda M et al., 1985) derived from a patient with Adult T cell leukemia/lymphoma. Preliminary analysis of the cell surface phenotype of C5MJ, ATL-2s and patient PH961 cells showed that C5MJ expresses CD4 and CD25 but not CD3, while ATL-2s did not express appreciable amounts of any of these matkers. On the other hand PBMC of the ATL patient PH961 expressed CD3 and CD25 in 100% of the cells and CD4 in 26% of the cells (Fig. 22). Results of confocal microscopy analysis are depicted in Figure 23. In all three HTLV-1 infected cells/ cell lines (C5MJ, ATL-2s and Ph961), HBZ was clearly detected by the 4D4-F3 mAb in the characteristic speckled-like structures in the nucleus. However, and importantly, both the intensity of fluorescence and the number of HBZ-positive cells was substantially different from the ones detected in 293T cells transiently transfected with HBZ (compare boxed panels in Fig. 23). Low intensity of fluorescence in C5MJ, ATL-2s and PH961 was expected as these cells are endogenously producing HBZ as results of their HTLV-1 infection and HTLV-1-dependent oncogenic transformation. More interestingly however was the fact that the percentage of HBZ positive cells detected as positive by the 4D4-F3 mAb were different for each cell type. The average of HBZ positive

cells was 75% for C5MJ, 100% for ATL-2s and 80% for PH961 cells, as assessed in at least three independent experiments (Fig. 23). This could be due to the detection threshold of our anti-HBZ antibody. Nevertheless these results clearly indicated that the expression of HBZ can substantially fluctuates even in HTLV-1 chronically infected or in ATLL patient-derived tumor cells.

4.7 Quantification of endogenous HBZ protein in HTLV-1 infected and in ATL tumor cells by the 4D4-F3 mAb.

It was further investigated whether the 4D4-F3 antibody could be used to estimate the amount of HBZ protein present in HTLV-1 infected and in ATL tumor cell lines. To this purpose a careful quantification of purified GST-tagged HBZ protein by western blotting was performed to assess the detection limit of the 4D4-F3 antibody and to construct a corresponding curve. As little as 3.12ng of HBZ protein could be detected by this approach (Fig. 24A). Subsequently western blot analysis of distinct dilutions of cell lysates from a fixed number of myc-tagged HBZ-transfected 293T cells was performed (Fig. 24B) and plotted the corresponding densitometry data on the curve constructed with the GST-tagged HBZ. This allowed us to define a provisional value of the amount of HBZ present in the transfected cells on a per cell basis by taking into account the percentage of HBZ transfected cells as shown in Figure 23. This value was $34{,}72x10^{-3}$ pg/cell, corresponding to $8x10^{5}$ molecules/cell (assuming a molecular weight of 36 kDa for myc-HBZ). Similar experiments were performed with cell lysates from C5MJ, ATL-2s and PH961 patient cells (Fig 24C). It must be stressed that in order to visualize by western blot specific HBZ bands in C5MJ, ATL-2s and PH961 cell lysates, it was necessary to process $50x10^{6}$ cells as compared to

$3x10^6$ HBZ-transfected 293T cells. Assuming a molecular weight of 26 kDa for endogenous HBZ, it was estimated that HBZ-positive C5MJ and ATL-2s cell lines contained an average of $1,04x10^{-3}$ pg/cell corresponding to 24.000 molecules/cell, and $1,56x10^{-3}$ pg/cell corresponding to 36.000 molecules/cell, respectively. In patient PH961 cells it was estimated an average of $0,78x10^{-3}$ pg/cell corresponding to 18.000 molecules/cell. Thus, with all the limitation of the analysis used, it was concluded that the amount of endogenously made HBZ molecules in freshly isolated ATL cells, in ATL cell line and in a chronically infected cell line was comparatively much lower (22-44 fold) than the amount observed in transiently transfected 293T cells.

4.8 Molecular interactions and cellular co-localizations between HBZ and cellular factors, in HBZ over-expressing 293T transfected cells and endogenously expressing HTLV-1 infected cells

It has been reported that HBZ can interact *in vivo* with several transcription factors (Usui T et al., 2008; Basbous J et al., 2003; Zhao T et al., 2009) and it has been hypothesized that this interaction may have functional importance for the pathological role played by HBZ in HTLV-1-infected patients (Barbeau B et al., 2013). However most of the experiments demonstrating HBZ-host factors interaction and co-localization have been carried out in cells over-expressing HBZ, mostly HBZ tagged with several easily identifiable markers against which antibodies are available. In addition, because of lack of appropriate higly purified and high affinity anti-HBZ antibody (most experiments in this line have been performed with an anti-HBZ rabbit antibody originally produced by Gaudray G et al., 2001), a careful analysis of the interaction-colocalization between HBZ and cellular factors was indeed prevented in

endogenously HBZ expressing cells such as HTLV-1 infected or ATL tumor cells. The 4D4-F3 anti-HBZ mAb was then used to assess the possible biochemical interactions and subcellular co-localizations of HBZ with cellular factors in ATL tumor cells and in C5MJ cells. We first checked the possible *in vivo* interaction between HBZ and two crucial nuclear factors such as JunD and CBP that are involved in several steps of both HTLV-1 replication and regulation of cellular gene expression. Cell extracts derived from C5MJ, ATL-2s and, from PBMC patient PH961 were first immunoprecipitated with the 4D4-F3 mAb and the resulting immunoprecipitate analyzed by SDS-PAGE and western blotting with specific antibodies for the presence of JunD and CBP. Results shown in Figure 25 indicate that endogenous HBZ interacts with both JunD and CBP (Fig. 25, lower panel), although to different extent depending on the cell analyzed and the amount of HBZ expressed. Indeed, both CBP and JunD interactions with HBZ were better detected in C5MJ and ATL-2s than in PH961 cells. This correlated with the higher amount of HBZ expressed in the first two cells compared to the patient ATL tumor cells. The overexpression of HBZ in 293T cells expressing endogenous CBP and JunD at levels comparable to HTLV-1 infected cells, resulted in a stronger interaction with both cellular factors, again suggesting that the limiting factor for the biological interactions was the concentration of HBZ present in the cell.

To further investigate the extent and the subcellular location of possible intracellular interaction between HBZ and cellular factors in HTLV-1 infected and ATL tumor cells, an extensive analysis by confocal microscopy was carried out. In this case the analysis included not only CBP and JunD but also other nuclear factors such as p300 and CREB-2, as well as nucleolin a marker of nucleoli. Figure 26 shows the results of such analysis in C5MJ, Figure 27 in ATL-2s , and Figure 28 in patient PH961 cells. For all three figures, in the first series of vertical panels is depicted the distribution of HBZ protein (red fluorescence), in the second

series of vertical panels the staining pattern of the various nuclear markers listed in each panel (green fluorescence) and in the third series of vertical panels the merged fluorescence. The fourth series of vertical panels depicts the peak fluorescence distribution along a single line section (ROI) of the corresponding markers to better define specific co-localizations. The fifth series of vertical panels shows the phase contrast image of the cell(s) analyzed. A common feature, irrespective of the cell analyzed, was that only part of HBZ spots colocalized with those of either one of the various markers analyzed. A relatively higher colocalization was observed between HBZ and CREB-2 in C5MJ and ATL-2s cell lines, although this was not the case in patient PH961 ATL tumor cells.

A second important feature was related to PH961 cells in which all markers showed a relatively lower expression compared to the two cell lines, probably reflecting the fact the immortalization and in vitro tumor growth induce a generalized overexpression of genes involved in the fine homeostasis of cell growth. Within the above mentioned limits, HBZ colocalized with CBP and p300 better in C5MJ than in ATL-2s. JunD was diffusely expressed in ATL-2s with respect to both C5MJ and patient PH961 cells, rendering difficult the appreciation of HBZ-JunD colocalization in ATL-2s cells. Instead a detectable colocalization between HBZ and JunD was observed in both C5MJ and patient PH961 cells. HBZ did not colocalize with nucleolin in any of the cells under study, indicating that the HTLV-1 viral protein was not a nucleolar protein.

5. DISCUSSION

HBZ is an important HTLV-1 viral oncogene that is strongly implicated in the neoplastic transformation leading to ATL (Matsuoka M et al., 2007). In contrast to Tax-1 oncogene, required to initiate neoplastic transformation, but not be to maintain the oncogenic process, HBZ is constantly found in ATL cells (Matsuoka M et al., 2013). For lack of suitable reagents, however, this expression has been assessed mostly at the level of HBZ mRNA, and mRNA may not be the best suitable marker for HBZ protein expression (Suemori K., 2009). In fact, previous reports have shown that HBZ in its protein form is scarcely produced in the infected cells and is not, or only marginally, discriminated from uninfected cells by HBZ specific CTLs (Suemori K., 2009) (Hilburn S., 2011). It is therefore extremely important to define its modality of expression, amount, localization and pattern of interaction with cellular factors during HTLV-1 infection and particularly in ATLL cells. The above parameters can be defined *in vivo* only by using tools that can evidence endogenous HBZ protein. Among these tools, specific monoclonal antibodies are certainly the most appropriate. Indeed, the use of the first described anti-HBZ mAb, 4D4-F3, specific for an epitope within the 97-135 aa region, has allowed us to characterize for the first time the expression and the localization of HBZ molecules in chronically infected HTLV-1 positive cells as well as in cells from an ATL patients, either as an established cell line (ATL-2s), or as fresh tumor cells from patient PMBC. Moreover, for the first time an estimation of the number of HBZ molecules expressed in HTLV-1 infected and ATL tumor cells could be obtained.

Naturally expressed HBZ protein localized in the nucleus with a similar speckle-like distribution as the one observed in cells transfected with tagged HBZ protein. However several previously described aggregates of nuclear HBZ were shown to be artifacts of chimeric proteins, particularly in the case of studies conducted with GFP-HBZ constructs.

These findings emphasize the usefulness of our anti-HBZ mAb to better define the intracellular pattern of expression of HBZ. Confocal microscopy analysis of C5MJ, ATL-2s and particularly PBMC of the PH961 ATL patient indicated that the vast majority of the cells expressed HBZ. The percentage of positive cells varied from 75% in C5MJ, to 80% in PH961 ATL patient cells, and virtually 100% in ATL-2s cells. The results obtained in fresh PBMC of the PH961 ATL patient are of interest since they indicate that not only the vast majority of the PBMC are ATL tumor cells but also that virtually all of them express HBZ protein. PH961 patient ATL cells displayed a cell surface phenotype with 100% of the cells coexpressing CD3 and CD25 molecules, compatible with a T cell-activated phenotype, although these cells were only 26% positive for CD4 and negative for CD8 cell surface molecules. Thus most of the leukemic cells did not present the phenotypic characteristics of regulatory T cells (Tregs, CD4+/CD25+) or effector/memory T cells supposed to be the major targets of HTLV-1-mediated cellular transformation (Karube K et al., 2004)(Satou Y et al., 2011) (Toulza F et al., 2008). More refined studies are presently underway to further clarify the phenotype and the possible functional correlates of CD3+/CD25+/CD4- and CD3+/CD25+/CD4+ cells in PH961 patient. It must be stressed, however, that also the cell surface phenotype of the ATL-2s cell line was rather peculiar, as ATL-2s cells were negative for CD3 and CD4 and expressed only a very limited amount of CD25 molecules (Figure 22).

The availability of 4D4-F3 mAb has allowed for the first time to estimate the number of HBZ molecules expressed on a per-cell basis in chronically infected C5MJ and in ATL tumor cells. In the three cells this number was far less (22 to 44 fold less) than the one expressed in HBZ-transfected cells such as 293T cells used by most investigators to characterize the pattern of expression, the co-localization and the possible interaction of HBZ with cellular factors. In absolute number C5MJ, ATL-2s and patient PH961 cells contained 24.000, 36.000 and

18.000 molecules per cell, compared to an average o 800.000 molecules observed in HBZ-transfected 293T cells. These results may help to better understand and evaluate the quantitative expression of HBZ during the various phases of HTLV-1 infection leading to chronic infection and eventually to neoplastic transformation.

Many nuclear factors have been reported to interact with HBZ. However most of these interactions were assessed in 293T or COS cells transfected with tagged HBZ, thus in HBZ overexpression conditions and in non physiological cellular models of HBZ expression. In this study we demonstrated that endogenous HBZ expressed in chronically infected and in ATL tumor cells interact *in vivo* with cellular transcription factors that are involved both in the control of HTLV-1 replication and in the host cell homeostasis. We could show that native HBZ can interact with CBP and JunD both in C5MJ and in the ATL tumor cells, although to different extent. In the two cell lines C5MJ and ATL-2s the interaction was consistently higher than the one observed in fresh ATL patient PH961 cells and partially correlated to the higher expression of HBZ protein in the former cell lines compared to the latter fresh tumor cells. These results definitively demonstrate that native HBZ can indeed interact *in vivo* with CBP and JunD in situations of "physiological" expression of the viral protein. Whether these interactions, as well as other described interactions such as the HBZ-CREB-2 and HBZ-p300, have a crucial functional role on the homeostasis of HTLV-1-infected cells and a causative implication in the cellular transformation leading to the ATL phenotype, it was not addressed in this study. Nevertheless, in C5MJ, ATL-2s and patient PH961 cells careful confocal microscopy analysis of co-localization of HBZ with either CBP, JunD, p300 or CREB-2 demonstrated a partial, often only a minor, colocalization between the viral protein and the cellular nuclear factors. Thus, possible functional correlates

of each single interaction of HBZ with the above nuclear factors in HTLV-1 infected and ATL cells should be framed within these findings.

In conclusion, the availability of the 4D4-F3 anti-HBZ mAb may significantly contribute to a better delineation of the role and presence of HBZ during HTLV-1 infection and cellular transformation.

6. FUTURE PERSPECTIVES

The severity of HTLV-1 infection is merely dictated by the underlying complex mechanism of infection involved. Although it is theorized that a cell to cell contact may be responsible for the spread of this infection, steps involved in HTLV-1 oncogenesis are yet to be fully understood. Understanding differential viral protein expression and their interaction/ localization with host factors in the infected cells would undoubtedly help in understanding different viral strategies to overcome immune response. Thus it becomes crucially important to study one of the key protein candidate involved in HTLV-1 infection, the HTLV-1 bZIP factor protein (HBZ). By generating the firstly reported anti-HBZ monoclonal antibody it will be feasible to detect and study HBZ protein in a detailed manner. Experiments done as a part of this PhD thesis project surely confirms the previously debated view of whether HBZ at protein level is expressed in the HTLV-1 infected cells or not. Further studies would focus on the interaction of HBZ protein with cellular factors in HTLV-1 infected cells. These experiments will show if the previously reported interaction of over-expressed HBZ (in transfected cells) with cellular factors are indeed of physiological relevance or not. Moreover, screening the leukemic cells from different patients, would show how many and which cell types are expressing HBZ protein. These studies can also be extended to cells from patients with HAM/ TSP or even asymptomatic carriers of HTLV-1 infection. All of the studies

mentioned above along with certain protein kinetics assay would throw light on the importance of HBZ in cellular transformation and maintenance of infectivity.

7. FIGURES

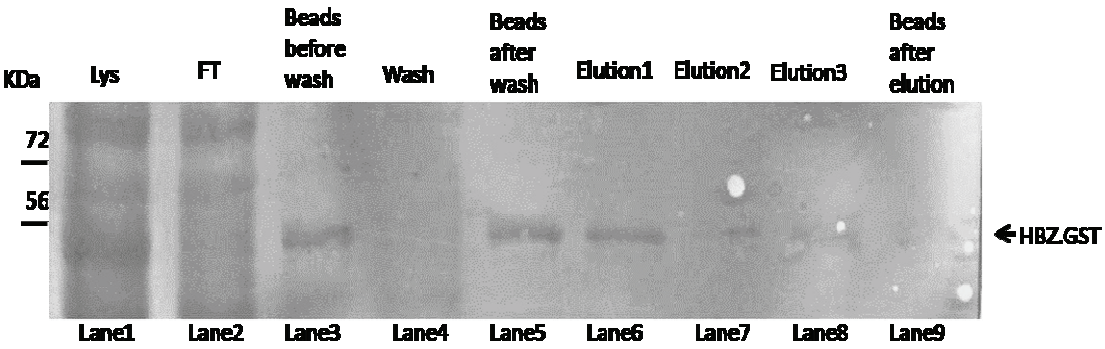

Figure 8: GST pull down assay

Rosetta cells transformed with pGEX2T-HBZ vector and induced to produce HBZ-GST were lysed and the fusion protein was collected by agarose glutathione beads. The final protein was eluted using reduced glutathione (10mM). The expected HBZ-GST band of 54 KDa could be seen in the eluted samples (lane 6,7,8) on a 8% SDS gel.

Lys – lysate, FT – flowthrough

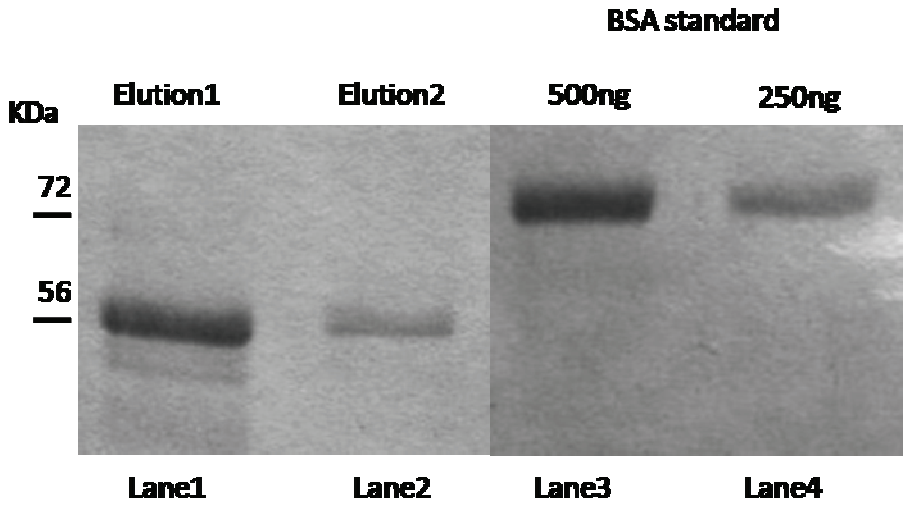

Figure 9: Protein Quantification by SDS-PAGE

The concentration of HBZ protein present in 10 µl of the elution 1 and 2 samples (total eluted volume 9ml) after agarose glutathione beads, was compared with know concentration of BSA standard protein. On this basis was constructed the BCA protein assay curve displayed in Figure 10.

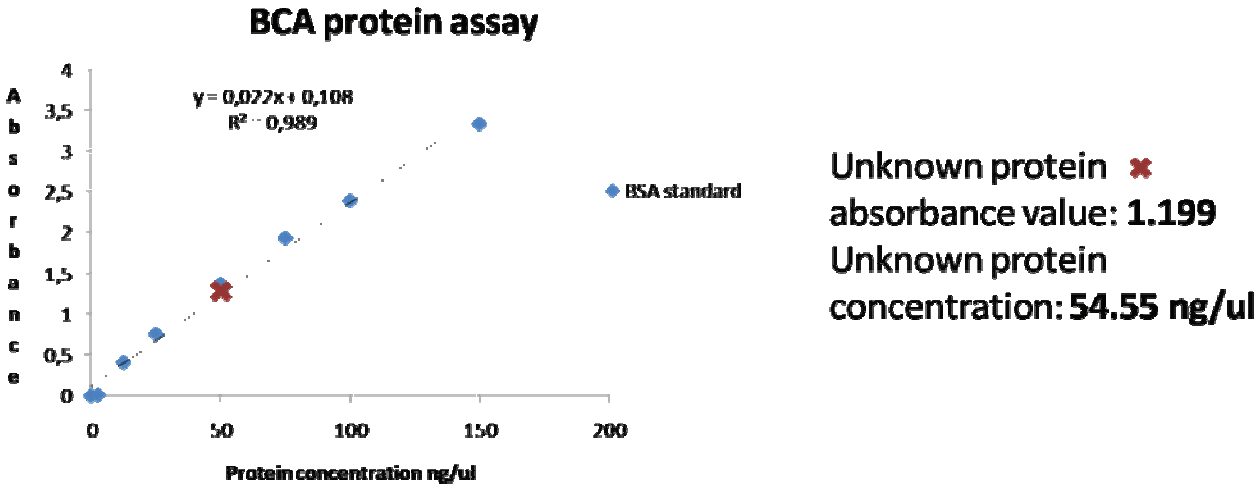

Figure 10: Protein Quantification by BCA assay

In order to quantify the amount of purified HBZ protein, a BCA protein assay was performed. Shown above in the figure is the plot for BSA standard (shown as blue diamond)

along with unknown purified HBZ.GST protein (shown as X) using BCA assay kit. Using the formula y=0.002x + 0.108 obtained from the plot, the unknown protein concentration was found to be 54.55 ng/ul (corresponding to an absorbance value of 1.199).

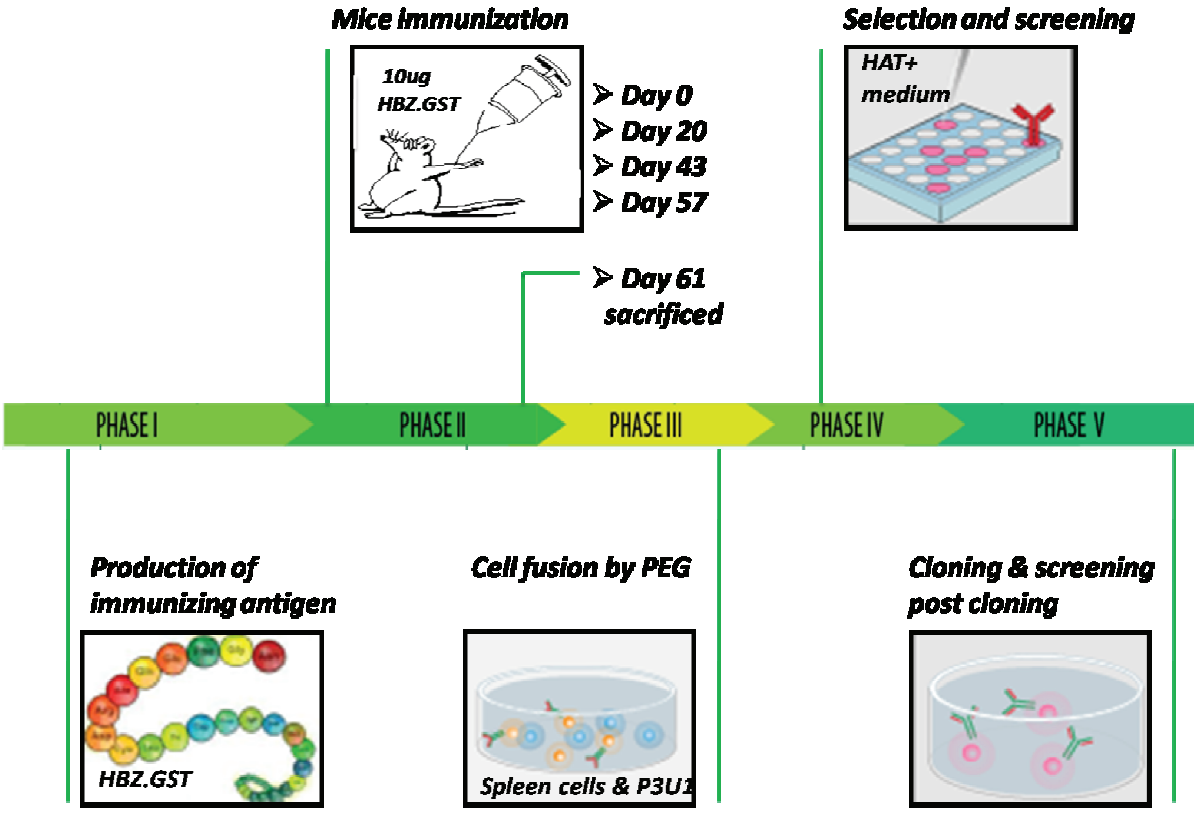

Figure 11: Monoclonal antibody generation scheme

Schematic for monoclonal antibody generation.

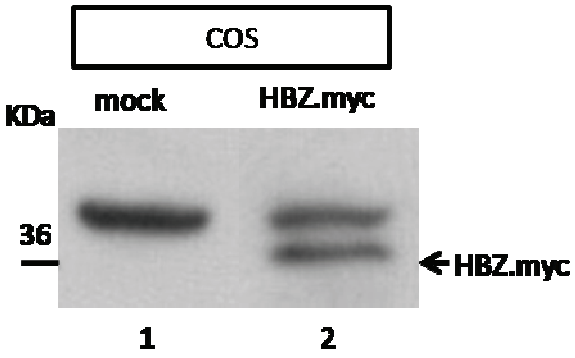

Figure 12: Readout for hybridoma screening

As a detection system for the anti-HBZ hybridomas, COS cells were transfected with 3 microgram of a DNA vector coding for HBZ.myc (pcDNA3.1HBZ.MycHis) and the cell lysate was used to screen different hybridomas. The cell lysate was first checked by western blot using an anti-myc (9E10) monoclonal antibody. The band at 36 Kda corresponds to HBZ.myc.

Lane1: COS cell lysate, Lane2: COS cell lysate expressing HBZ.myc

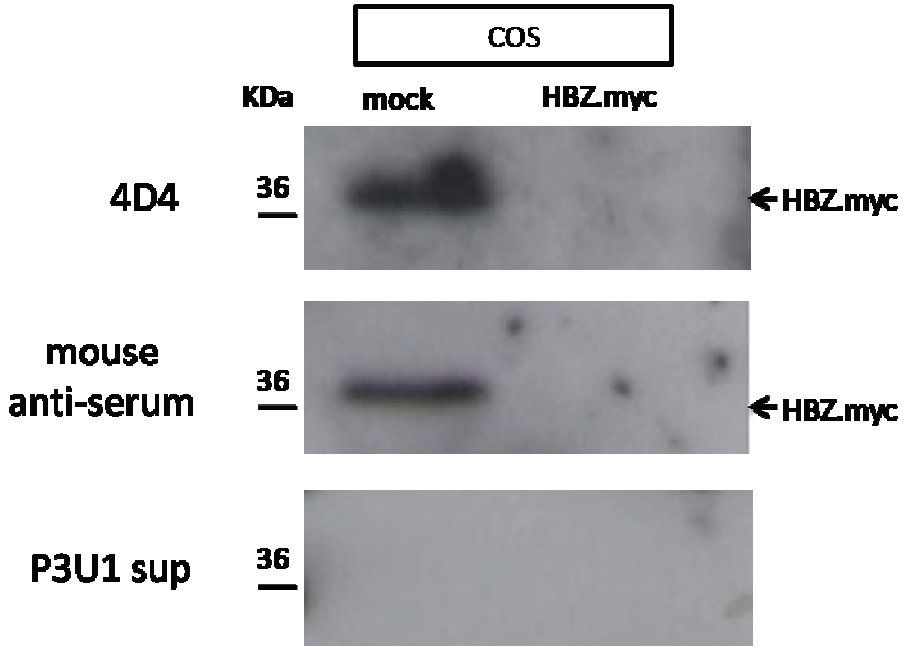

Figure 13: Hybridoma screening by western blot

The hybridoma supernatant were screened for anti-HBZ positivity by western blot, on membranes pre-transferred with myc-tagged HBZ protein. COS cells were transfected with 3ug of pcDNA3.1HBZ.myc vector (HBZ.myc) or with pcDNA3 vector alone (mock), and the

corresponding cell lysates (materials and methods) were used to check hybridoma supernatant. A total of 96 hybridoma supernatant were tested in the same way.

4D4: supernatant from one of many hybridomas tested after fusion

Mouse anti-serum: serum from immunized (HBZ-GST) mice as positive control

P3U1 sup: supernatant from P3U1 myeloma cells used to fuse the spleen cells as negative control

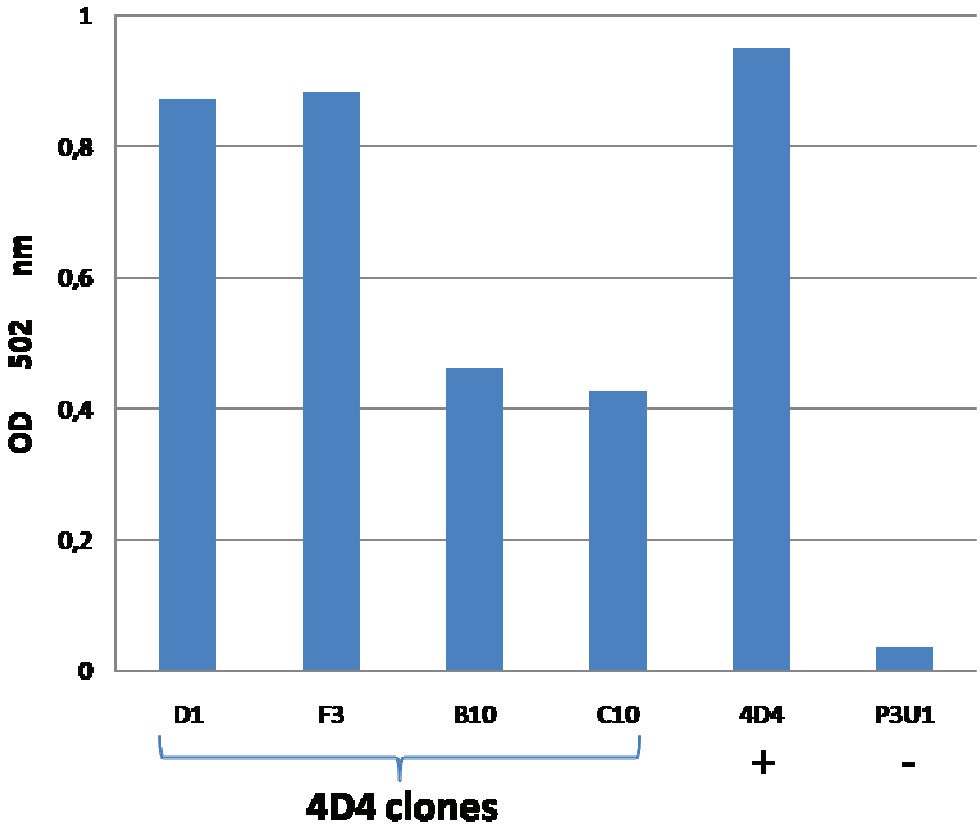

Figure 14: Screening of cloned hybridomas from 4F4 parental hybrid by ELISA

The anti-HBZ positive hybridoma 4D4 was cloned by serial dilution in a 96 well plate. The clones were maintained in HAT selection. The clones' supernatant was analyzed by ELISA using plates coated with purified HBZ-GST antigen and processed as described in materials and methods. The color developed was read with a spectrophotometer at 502 nm. Clones

represented here are with high (D1 & F3) and medium (B10 & C10) absorbance values. 4D4: positive control, P3U1: negative control.

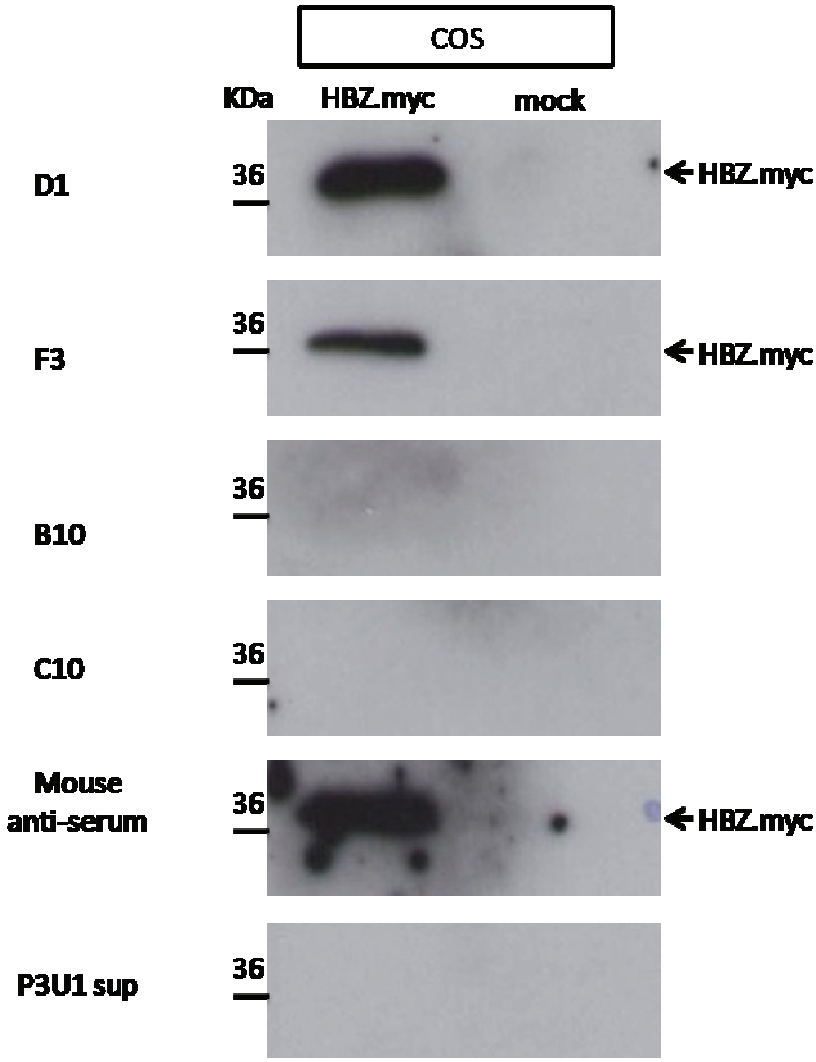

Figure 15: Confirming ELISA results by western blot

To confirm the ELISA results, supernatant from hybridoma clone that showed a high and medium absorbance were tested by western blot to detect HBZ.myc. Supernatant were diluted 1:1 in 5% milk in PBS1X.

D1 & F3, B10 & C10: 4D4 clones with high and medium absorbance value respectively by ELISA

Mouse anti-serum: serum from immunized mice as positive control

P3U1 sup: supernatant from P3U1 myeloma cells used to fuse the spleen cells as negative control

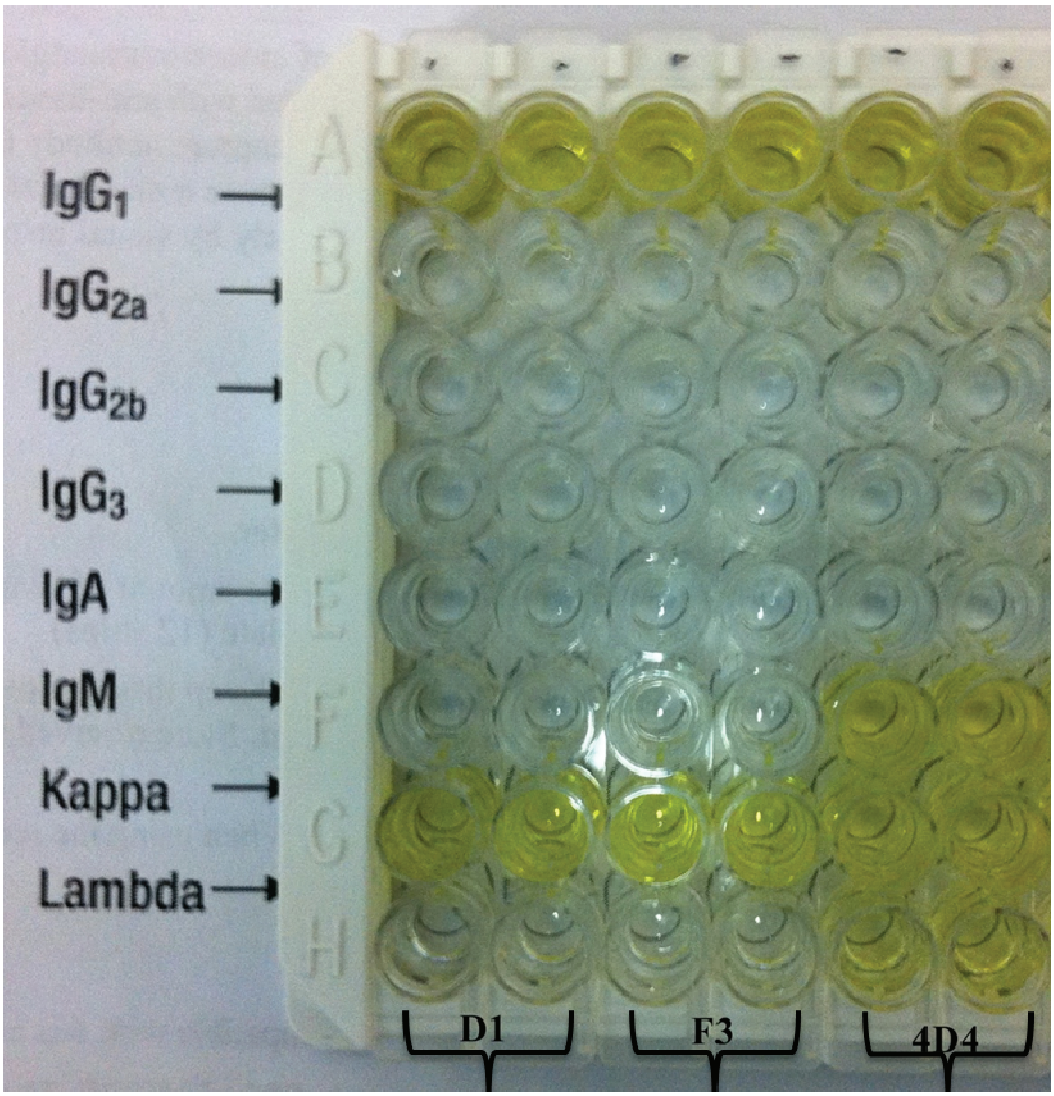

Figure 16: Antibody Isotyping by ELISA kit

The anti-HBZ parental hybridoma 4D4 and its derived D1 and F3 clones were isotyped by using an ELISA kit according to the manufacturer's instructions. All the samples were checked in duplicates. Yellow color indicates positivity for the corresponding type and subtype.

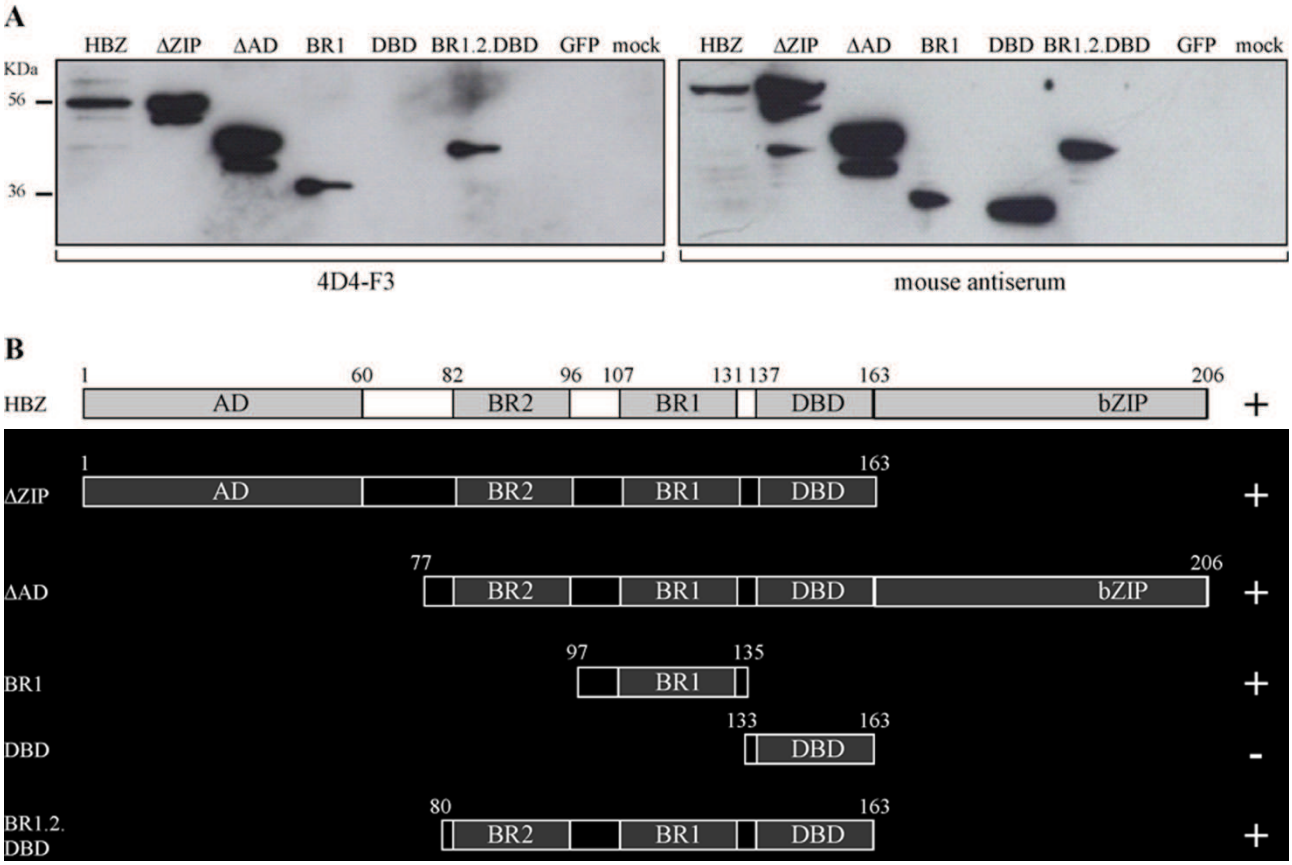

Figure 17: Epitope assignment of 4D4-F3 anti-HBZ mAb

A) Western blot analysis of full length GFP-tagged HBZ (HBZ) and a series of GFP-tagged HBZ fragments listed in the top of the left and right panels. Briefly, 293T cells were transfected with the various encoding GFP-HBZ cDNAs, with empty plasmid (mock) or with GFP cDNA (GFP). Twenty four hours after transfection cell lysates were prepared and analyzed by western blotting using the 4D4-F3 anti HBZ mAb (left panel) or the anti-HBZ antiserum prepared from the same animal used for somatic cell fusion (right panel). B)- Schematic representation of the same results depicted in A. The various HBZ constructs are listed on the left side followed by bars representing size and regions of the specific fragment analyzed. Numbers indicate the specific aminoacid position in the various fragments. Plus (+) and minus (-) symbols indicate positive or negative reactivity, respectively, of the 4D4-F3 mAb. Abbreviations: AD, activation domain; BR1, basic region 1; BR2, basic region 2; DBD, DNA binding domain; bZIB, b zipper domain.

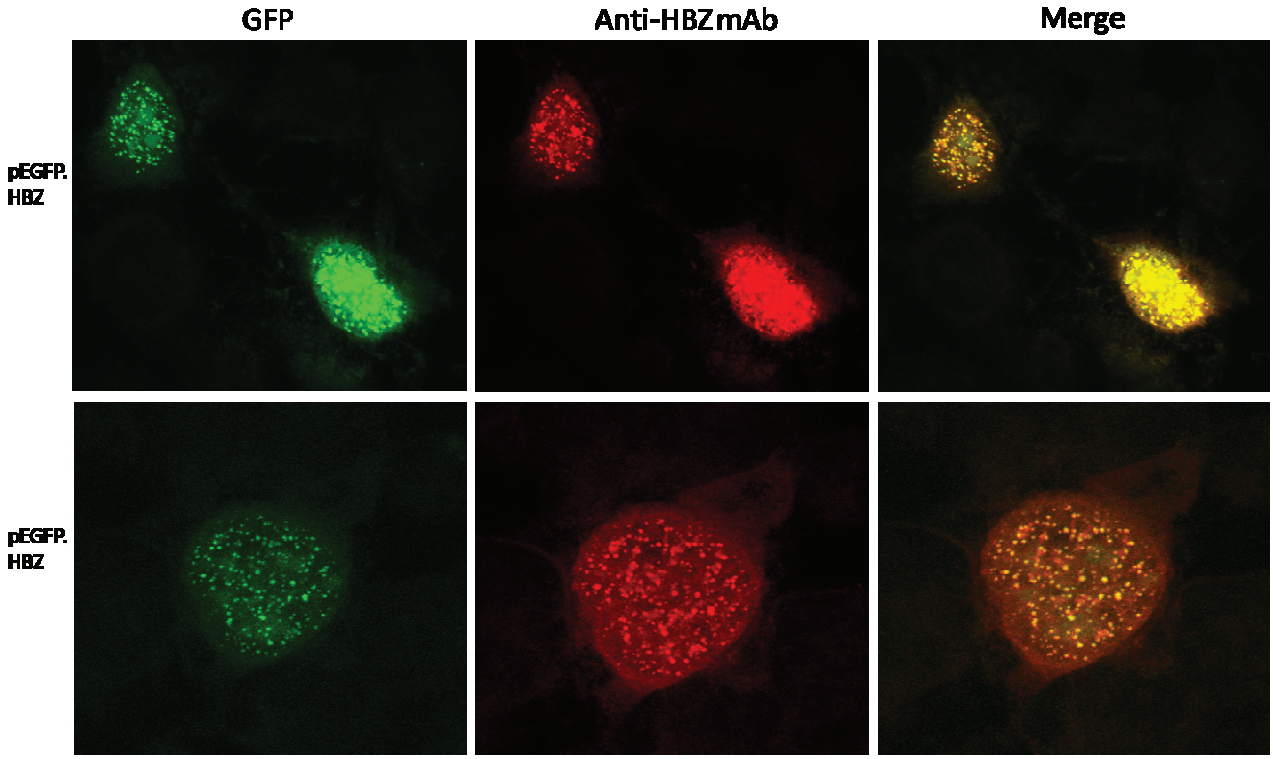

Figure 18: Anti-HBZ mAb detects exogenous HBZ in nuclear speckles

293T cells were transfected with 1 ug of pEGFP-HBZ-SP1 vector and processed as explained in materials and methods. Supernatant of anti-HBZ hybridoma 4D4.F3 was used as a primary antibody followed by Alexa flour 546 goat anti-mouse IgG (BD) as secondary antibody. The green color (GFP column) represents GFP protein fluorescence and red color (Anti-HBZ mAb column) represents HBZ protein-specific fluorescence as detected by the abovementioned secondary antibody. Merge column represents merging of red and green color.

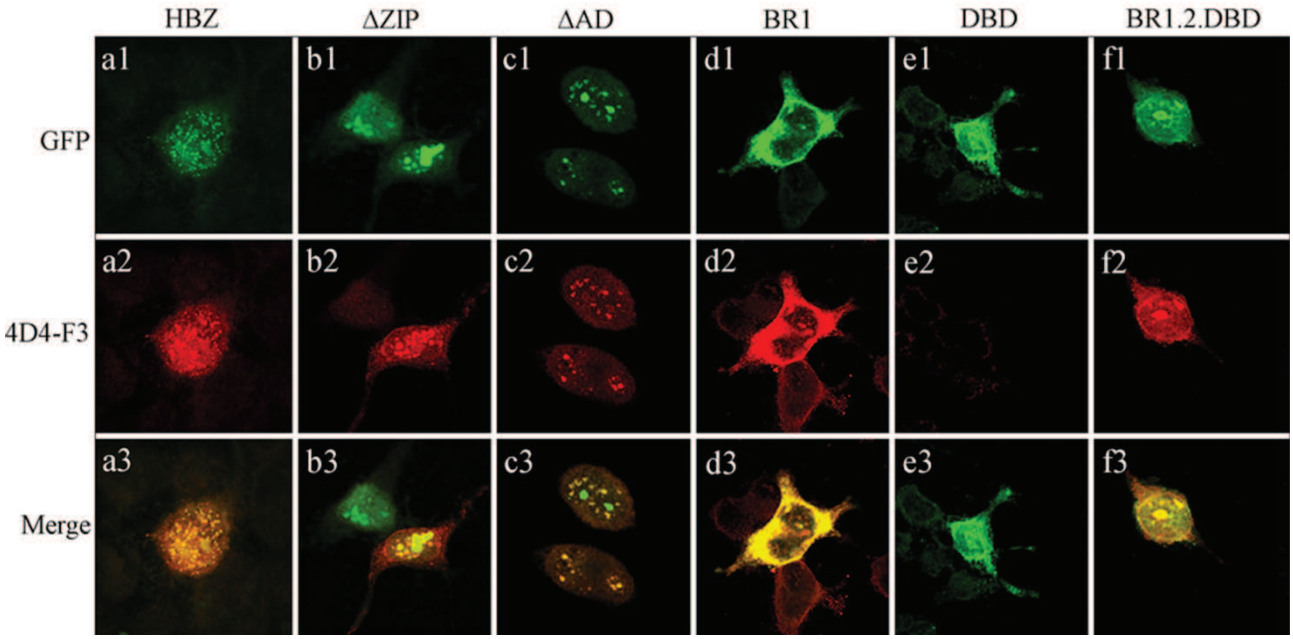

Figure 19: Localizing different HBZ constructs in transfected cells

Localization of full length HBZ and fragments as assessed by the 4D4-F3 mAb. Full length GFP-tagged HBZ (HBZ) and a series of GFP-tagged HBZ fragments listed in the top of the figure, were transfected in to 293T cells and their subcellular localization investigated in confocal microscopy either by GFP fluorescence (first series of horizontal panels) or by reactivity with the 4D4-F3 mAb followed by Alexa fluor 546-labeled goat anti-mouse antibody (second series of horizontal panels). Third series of horizontal panels represent the merge between the GFP and the Alexa fluor 546 signals.

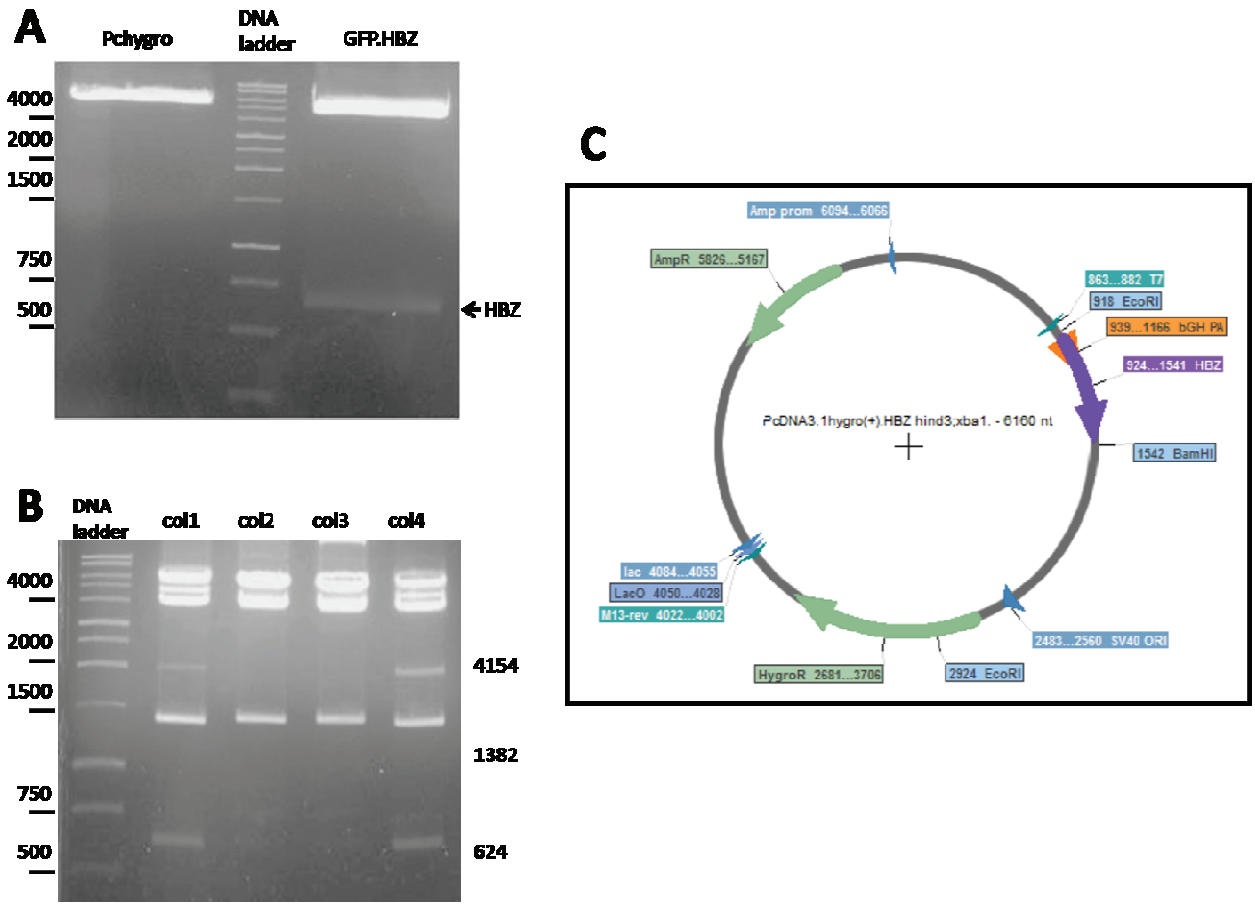

Figure 20: Generation of untagged HBZ mammalian expression vector

A DNA vector coding for only HBZ without any tag was generated as explained in materials and methods. **A**: Agarose gel electrophoresis of pcDNA3.1hygro and pEGFPc2.HBZ DNA vector doubly digested by XbaI and HindIII. HBZ fragment of 624 nucleotides is shown by arrow. **B**: Agarose gel electrophoresis of the ligation product (pcDNA3.1hygro.HBZ) post double restriction by EcoRI and BamH1. Two different vector:insert ratio (1:5 and 1:10) were used and two colonies from each were selected for restriction check (col1 & 2, col 3 & 4 respectively). The three expected DNA products post restriction are mentioned on right side. **C**: DNA map of the expected ligation product pcDNA3.1hygro.HBZ. Note that this vector has two EcoRI site and one BamH1 site.

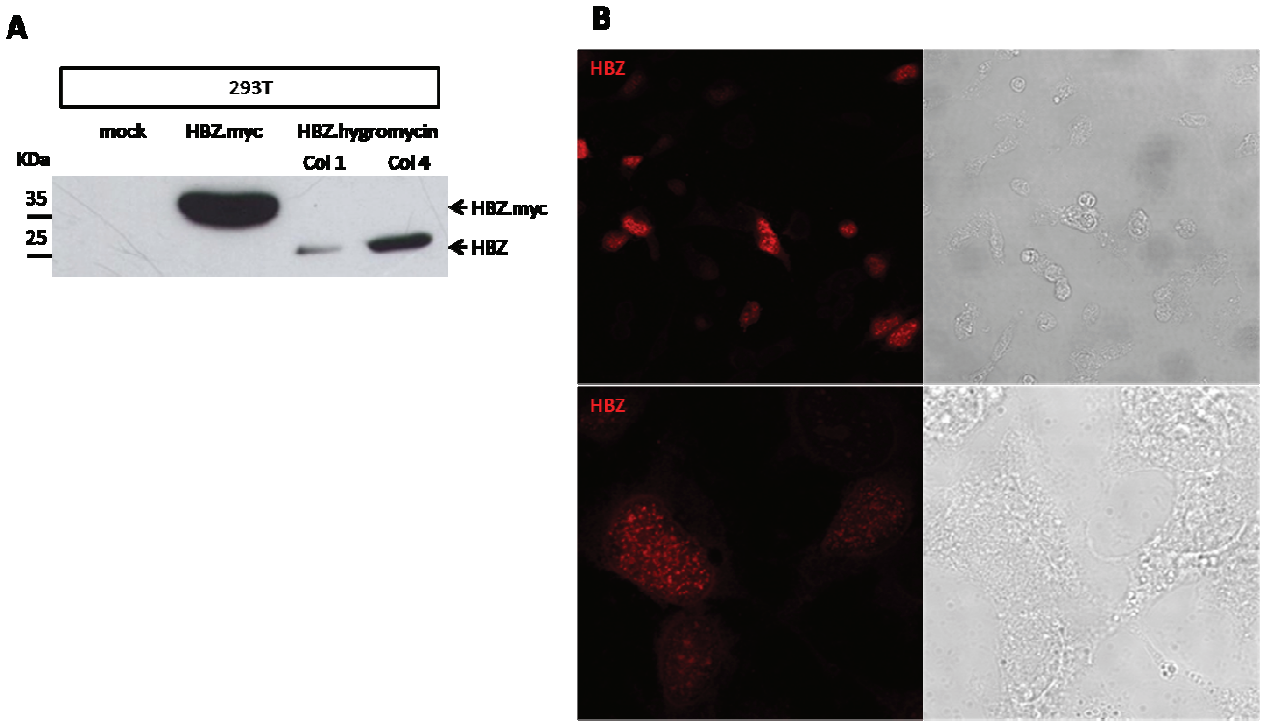

Figure 21: HBZ protein level in 293T cells transfected with pcDNA3.1hygro.HBZ vector

The newly generated pcDNA3.1hygro.HBZ vector was checked for protein expression by western blot and confocal microscopy. **A:** 293T cells were transfected with 3 ug of DNA vector coming from ligation product positive for double restriction check as explained in Fig 20. As a control, cells were also transfected with HBZ.myc vector. The cell lysate was prepared and subjected to western blot as described in materials and methods. The anti-HBZ monoclone 4D4.F3 was used as primary antibody. HBZ protein expressed alone runs slightly above 25KDa. **B:** 293T cells were transfected with 1ug of pcDNA3.1hygro.HBZ (1:5 ligation product) and the slides were prepared as explained in materials and methods. The anti-HBZ monoclone 4D4.F3 was used as primary antibody. The top and bottom panel show zoomed out and zoomed in views of HBZ-positive cells respectively.

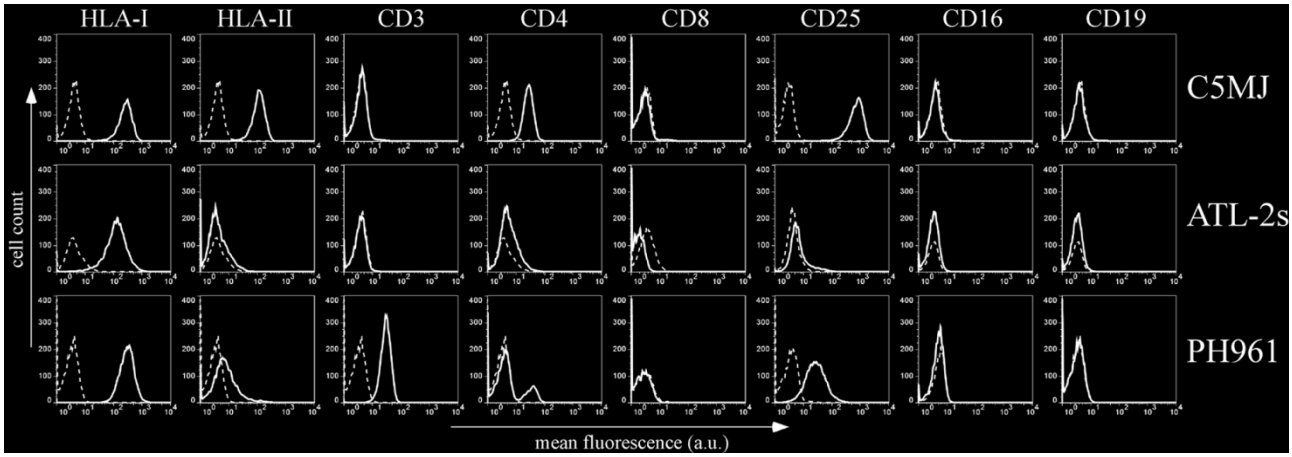

Figure 22: Cell surface phenotype of C5MJ, ATL-2s and patient PH961 cells

Cell surface phenotype of C5MJ, ATL-2s cell lines and of peripheral blood mononuclear cells from ATL patient PH961 was assessed by immunofluorescence and flow cytometry. The various cell surface markers listed in the top right of each histogram were assessed by specific monoclonal antibodies either directly labeled with fluorochromes (CD3, CD4, CD8, CD25, CD19, and CD16), or unlabeled (HLA class I and HLA class II DR) followed by FITC-labeled rabbit anti-mouse IgG. Specific fluorescence is represented by the bold histogram; negative isotype control is represented by the thin histogram. Values are expressed in the abscissa as mean fluorescence in arbitrary units (a.u.).

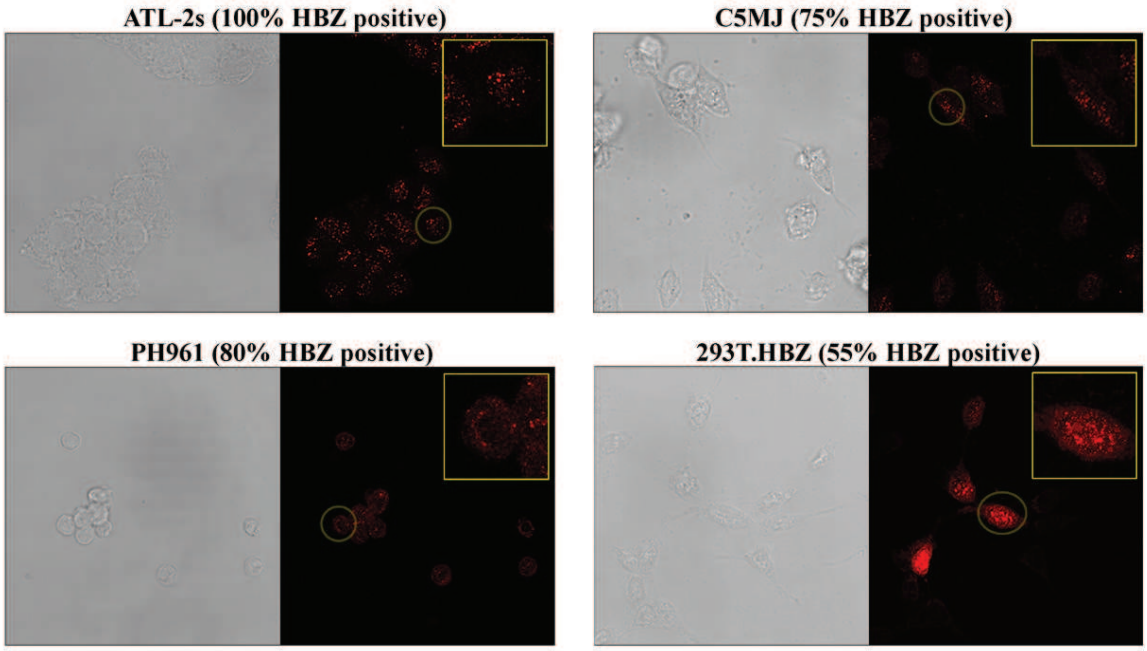

Figure 23: Expression and localization of endogenous HBZ in HTLV-1 chronically infected and in ATL tumor cells

C5MJ (HTLV-1 chronically infected), ATL-2s (ATL tumor cell line) and PH961 (PMBC of an ATL patient) were stained with the 4D4-F3 antibody, followed by Alexa fluor 546-labeled goat anti-mouse antibody and analyzed by confocal microscopy. 293T cells transiently transfected with myc-HBZ cDNA plasmid were used as comparison. Differential interference contrast image of each cell field analyzed is shown in the left side of each confocal picture. The small round yellow shade points to a HBZ positive cell shown enlarged in the yellow square insert. In parenthesis the percentage of HBZ-positive cells calculated by counting at least 200 cells.

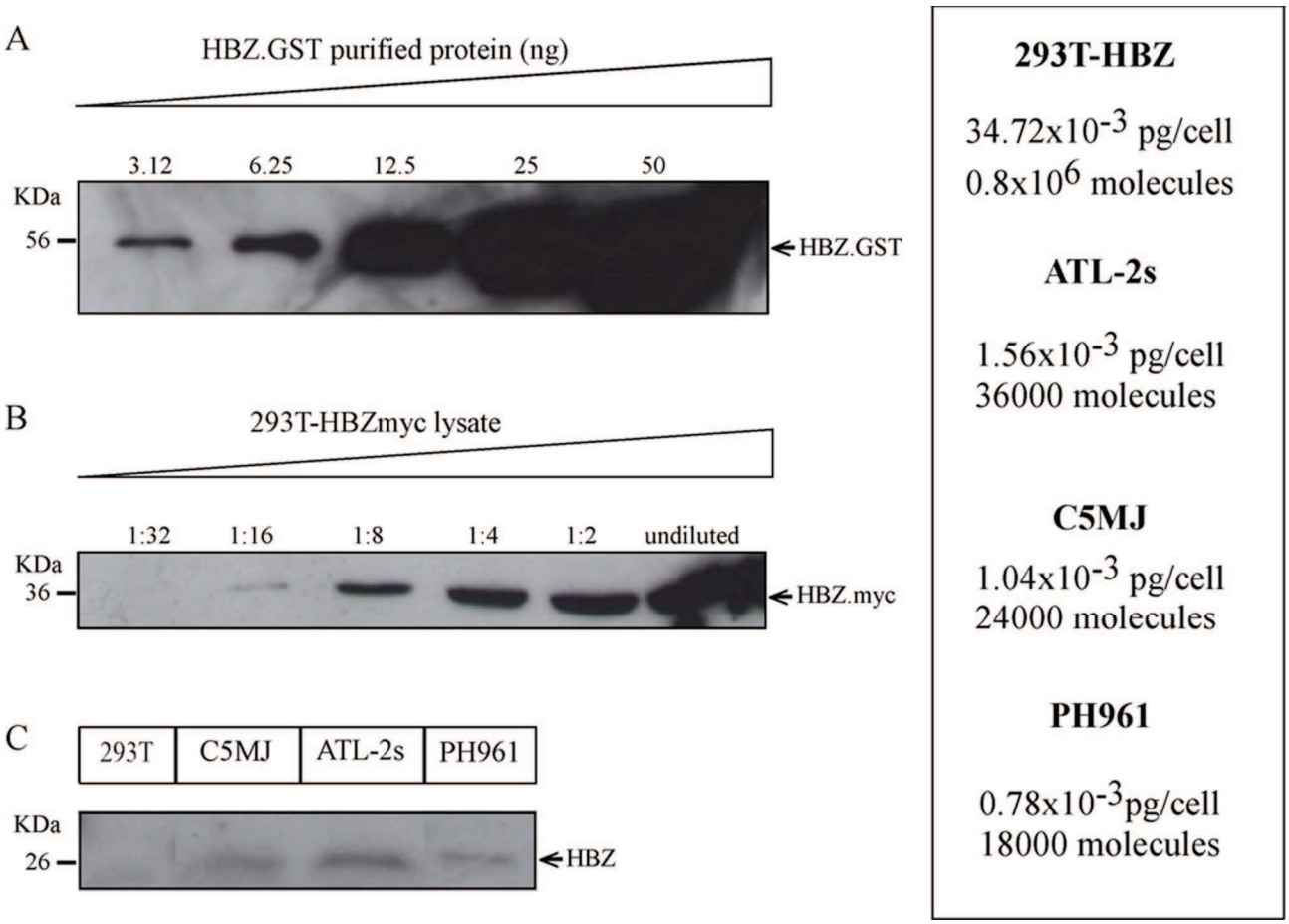

Figure 24: Quantification of endogenous HBZ expression in HTLV-1 chronically infected and in ATL tumor cells

In all panels, HBZ protein was migrated in SDS-PAGE gels. After blotting onto nitrocellulose membranes, HBZ protein was detected by 4D4-F3 mAb followed by HRP conjugated anti-mouse antbody A)- Purified GST-tagged HBZ protein at different nanogram (ng) concentration was used to construct a detection curve . B)- Western blots of serial dilutions of cell lysate from 293T cells transfected with myc-tagged (HBZ.myc). In this experiment 3µg of HBZ.myc were transfected in 5 million cells. After transfection, cells were lysed in 1ml of lysis buffer and 40 µl of cell lysate, either undiluted or diluted as listed, used for western blotting. C)- Western blots of cell lysate from C5MJ, ATL-2s, and PH961 patient ATL tumor cells. In this experiment 50 million cells were lysed in 2ml of lysis buffer and 40 µl of undiluted cell lysate used for western blotting.

In the right side insert of the Figure are listed the calculated values of HBZ picograms (pg) per cell and the deduced number of HBZ molecules per cells. For further details see the text.

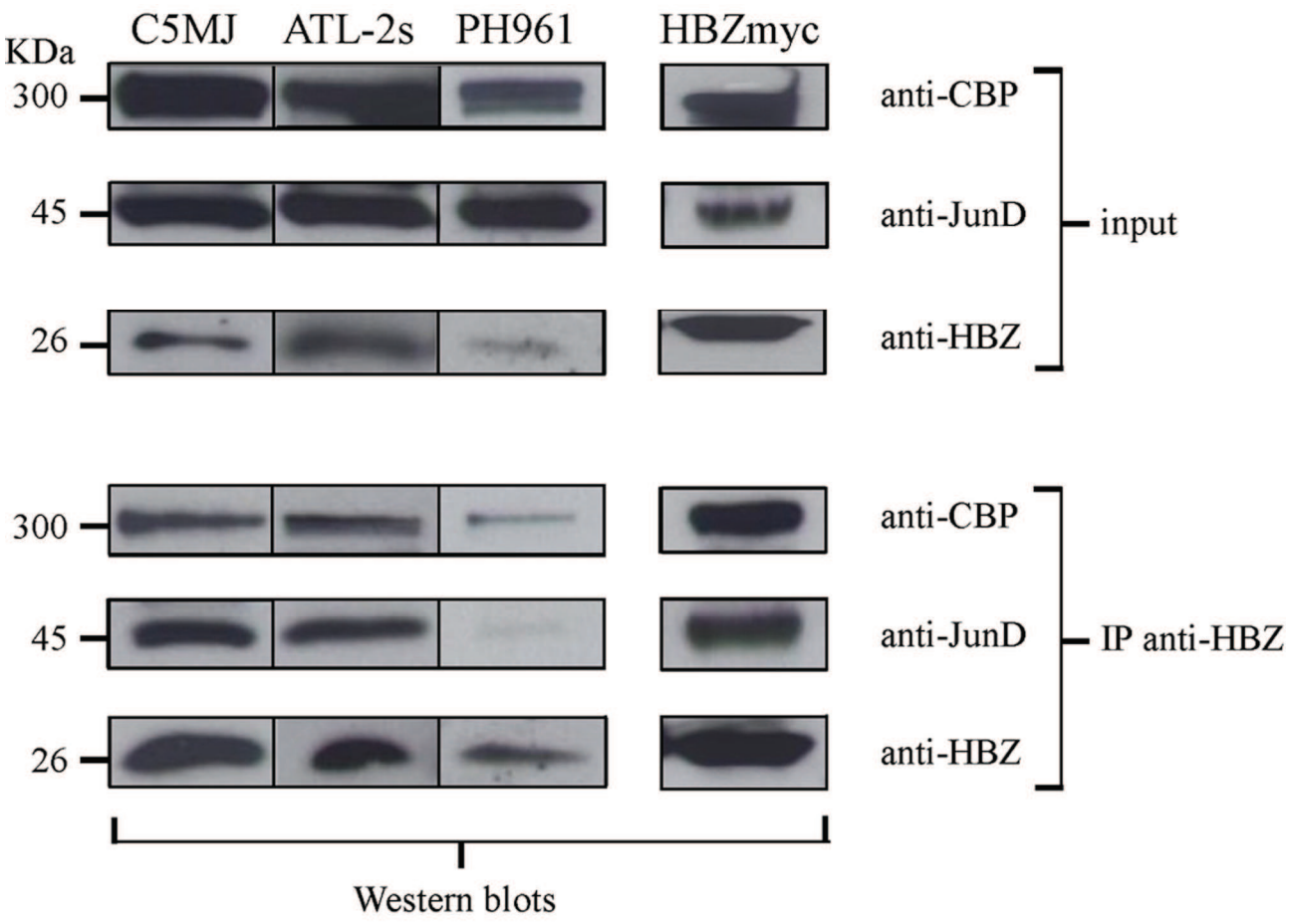

Figure 25: ***in vivo*** **interaction of endogenous HBZ with intracellular molecules.**

The possible in vivo interaction between endogenous HBZ and CBP or JunD was assessed by co-immunoprecipitation assay. Lower panel: cell lysates from 50 million cells of C5MJ, ATL-2s or PH961 ATL patient, prepared as described in the legend to Figure 4, were immunoprecipitated by using HBZ covalently linked to CNBr-activated Sepharose 4B beads (IP anti-HBZ). After elution from HBZ-Sepharose 4B beads, the eluted material was migrated on SDS-PAGE gels, blotted on nitrocellulose membranes and probed with antibodies specific for either anti-CBP, anti-JunD or with the 4D4-F3 mAb (anti-HBZ). Upper panel: prior immunoprecipitation 40 µl of cell lysate were used to assess the presence of the specific protein by western blot (input).

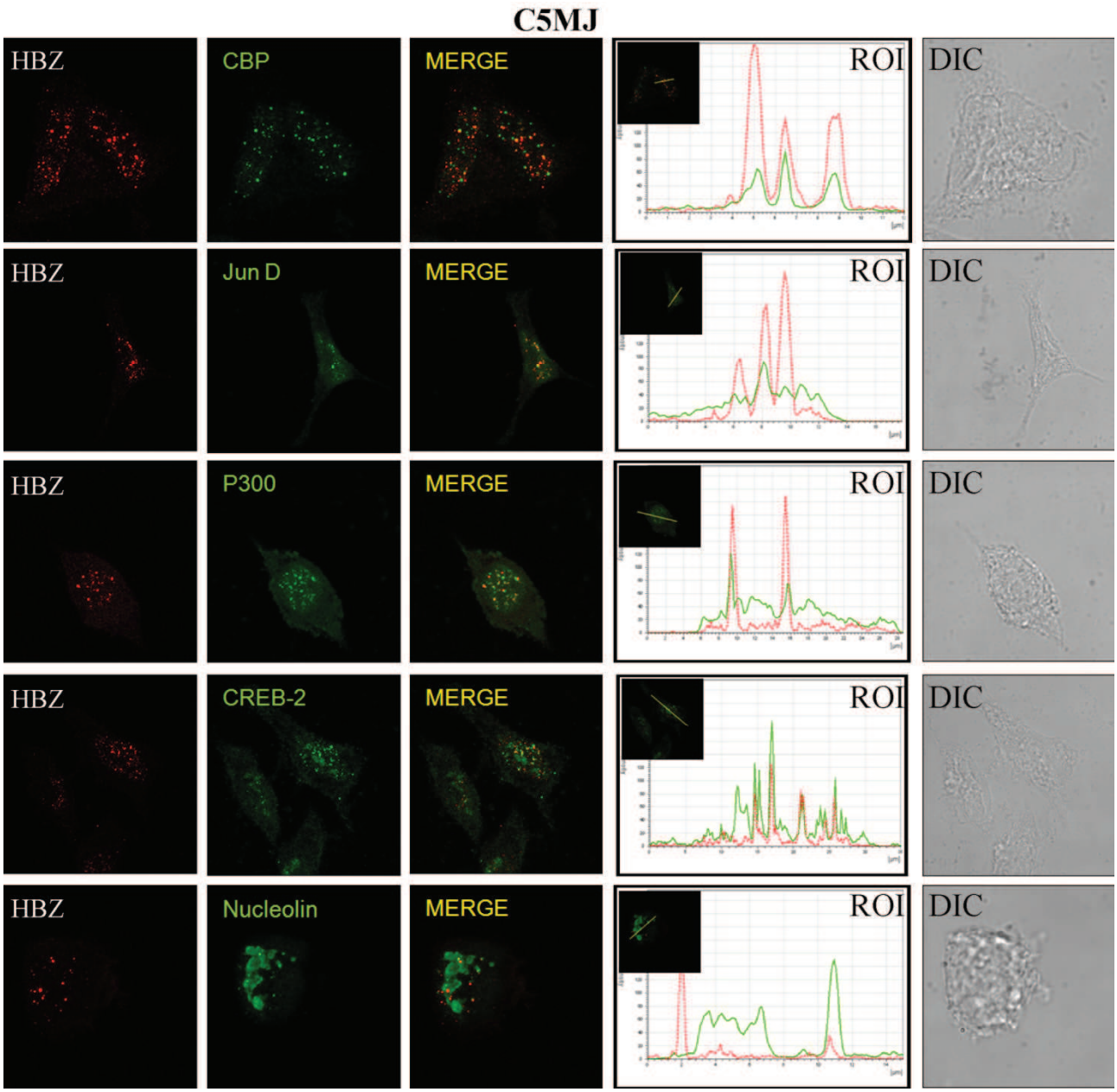

Figure 26: Co-localization of endogenous HBZ with intracellular factors in C5MJ cells

C5MJ cells were reacted in a pairwise combination with the 4D4-F3 anti HBZ mAb antibody, and either polyclonal rabbit anti-CBP, anti-JunD, anti p300, anti CREB2, or anti nucleolin antisera. Anti-HBZ mAb was revealed by Alexa fluor 546-labeled goat anti-mouse IgG (red), whereas the other rabbit antisera were revealed by Alexa fluor 488-labeled goat anti-rabbit antibodies (green). The MERGE column panels represent the merge between the Alexa fluor 546 and the Alexa fluor 488 signals. A colocalization of HBZ with either one of the intracellular factors results in a yellow colour. The reference of intensity (ROI) drawn along mid-nucleus level of the merge image (insert) is represented by red and green peaks in

the histogram (red for HBZ and green for the intracellular factor). Differential interference contrast (DIC) image of each cell field analyzed is shown in the last vertical series of panels.

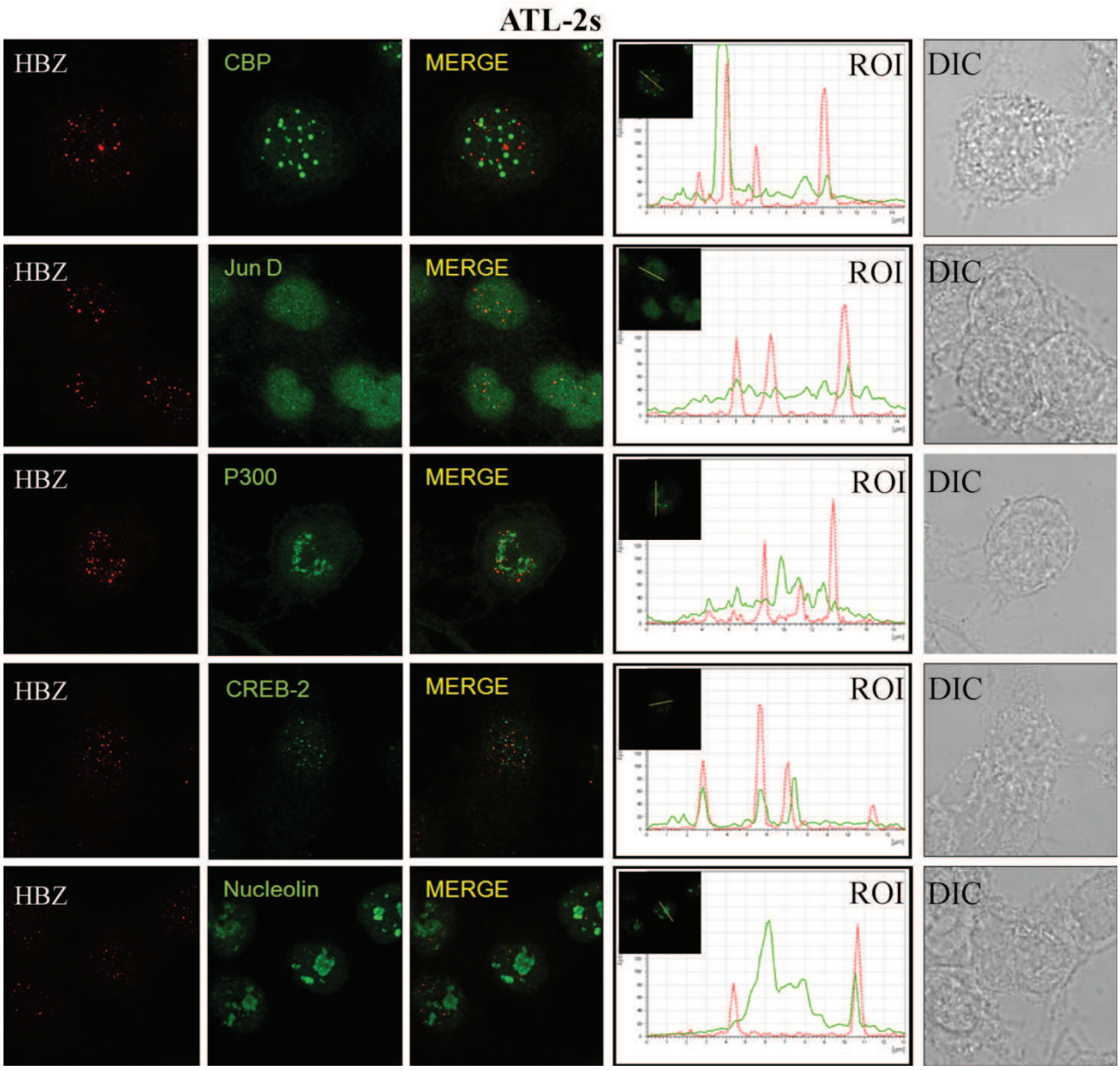

Figure 27: Co-localization of endogenous HBZ with intracellular factors in ATL-2s cells

ATL-2s cells were reacted in a pairwise combination with the 4D4-F3 anti HBZ mAb antibody, and either polyclonal rabbit anti-CBP, anti-JunD, anti p300, anti CREB2, or anti nucleolin. For detection and other relevant informations see the legend to Figure 26.

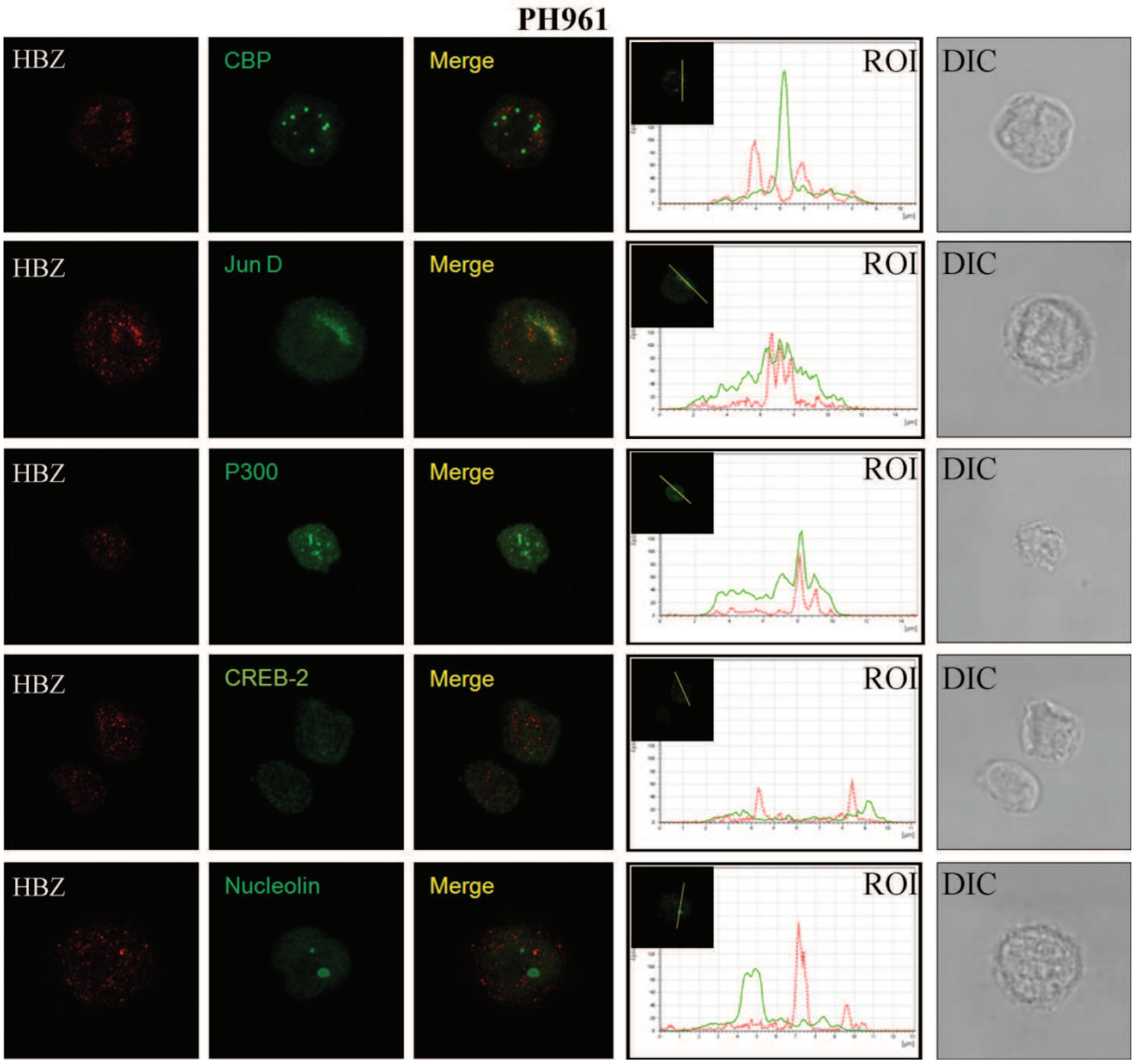

Figure 28: Co-localization of endogenous HBZ with intracellular factors in PH961 cells

PH961 patient cells were reacted in a pairwise combination with the 4D4-F3 anti HBZ mAb antibody, and either polyclonal rabbit anti-CBP, anti-JunD, anti p300, anti CREB2, or anti nucleolin. For detection and other relevant informations see the legend to Figure 26.

8. Reference

Accolla RS, Carrel S, Mach J P. Monoclonal antibodies specific for carcinoembryonic antigen and produced by two hybrid cell lines. Proc Natl Acad Sci USA; 77:563-566 (1980).

Arisawa K, Soda M, Endo S, Kurokawa K, Katamine S, Shimokawa I, Koba T, Takahashi T, Saito H, Doi H, Shirahama S. Evaluation of adult T-cell leukemia/lymphoma incidence and its impact on non-Hodgkin lymphoma incidence in southwestern Japan. Int J Cancer, 85:319-324 (2000).

Arnold J, Yamamoto B, Li M, Phipps A J, Younis I, Lairmore M D. Enhancement of infectivity and persistence invivo by HBZ, a natural antisense coded protein of HTLV-1. Blood 107, 3976–3982.doi: 10.1182/blood-2005-11-4551 (2006).

Arnold J, Zimmerman B, Li M, Lairmore M D, Green P L, Human T-cell leukemia virus type-1 antisense-encoded gene, Hbz, promotes T-lymphocyte proliferation. Blood, 112, 3788–3797 (2008).

Bangham CR and Osame M. Cellular immune response to HTLV-1. Oncogene, 24: 6035-6046 (2005).

Bangham CR. The immune response to HTLV-1. Curr. Opin. Immunol., 12, 397–402 (2000).

Barbeau B and Mesnard J M. Does the HBZ gene represent a new potential target for the treatment of adult T-cell leukemia? Int. Rev. Immunol.26, 283–304 (2007).

Barbeau B, Peloponese J M, Mesnard J M. Functional comparison of antisense proteins of HTLV-1 and HTLV-2 in viral pathogenesis. Front. Microbiol. 4:226 10.3389/fmicb.2013.00226 (2013).

Basbous J, Arpin C, Gaudray G, Piechaczyk M, Devaux C, Mesnard J M. HBZ factor of HTLV-I dimerizes with transcription factors JunB and c-Jun and modulates their transcriptional activity. J. Biol. Chem., 278, 43620–43627 (2003).

Bhigjee AI and Hlela C. HTLV-1 infection and disease with special reference to the dermatological manifestations - a critical review. OA Dermatology. Jan 18;2(1):1 (2014).

Cavanagh M H, Landry S, Audet B, Arpin-Andre C, Hivin P, Paré M E, Thete J, Wattel E, Marriott S J, Mesnard J M. HTLV-I antisense transcripts initiating in the 3'LTR are alternatively spliced and polyadenylated. Retrovirology, 3, 15 (2006).

Clerc I, Hivin P, Rubbo P A, Lemasson I, Barbeau B and Mesnard J M. Propensity for HBZ-SP1 isoform of HTLV-I to inhibit c-Jun activity correlates with sequestration of c-Jun into nuclear bodies rather than inhibition of its DNA-binding activity. Virology 391, 195–202.doi: 10.1016/j.virol.2009.06.027 (2009).

Clerc I, Polakowski N, AndreArpin C, Cook P, Barbeau B, Mesnard J M. An interaction between the human T cell leukemia virus type1 basic leucine zipper fac- tor (HBZ) and the KIX domain of p300/CBP contributes to the down- regulation of tax-dependent viral transcription by HBZ. J. Biol.Chem. 283, 23903–23913.doi:10.1074/jbc. M803116200 (2008).

Cook P R, Polakowski N and Lemasson I. HTLV-1 HBZ protein deregulates interactions between cellular factors and the KIX domain of p300/CBP. J. Mol. Biol. 409, 384–398.doi:10.1016/ j.jmb.2011.04.003 (2011).

Cooper S A, Schim van der Loeff M, Taylor G P. Practical Neurology,9:16-26 (2009).

EnoseAkahata Y, Abrams A, Massoud R, Bialuk I, Johnson KR, Green P L . Humoral immune response to HTLV-1 basic leucine zipper factor (HBZ) in HTLV- 1 infected individuals. Retrovirology 10, 19.doi:10.1186/1742-4690- 10-19 (2013).

Franchini G, Fukumoto R & Fullen J R. T-cell control by human T-cell leukemia/lymphoma virus type 1**,** Tax protein of HTLV-1 inhibits CBP/p300-mediated

transcription by interfering with recruitment of CBP/p300 onto DNA element of E-box or p53 binding site. Int. J. Hematol. 78**,** 280–296 (2003).

Franklin A A and Nyborg JK. Mechanisms of Tax regulation of human T cell leukemia virus type I gene expression, J. Biomed. Sci. 2**:**17-29 (1995).

Gaudray G, Gachon F, Basbous J, Biard-Piechaczyk M, Devaux C, Mesnard J M. The complementary strand of HTLV-1 RNA genome encodes a bZIP transcription factor that down-regulates the viral transcription. J. Virol., 76, 12813–12822 (2002).

Gessain A and Mahieux R. A virus called HTLV-1. Epidemiological aspects. Presse med. 29(40):2233-9 (2000).

Hidaka M, J Inoue, M Yoshida and M Seiki. Post-transcriptional regulator (rex) of HTLV-1 initiates expression of viral structural proteins but suppresses expression of regulatory proteins. EMBO J. 7**:**519-523 (1988).

Higuchi I, Montemayor ES, Izumo S, Inose M, Osame M. Immunohistochemical characteristics of polymyositis in patients with HTLV-I-associated myelopathy and HTLV-I carriers. MuscleNerve, 16: 472-476 (1993).

Hilburn S, Rowan A, Demontis MA. In vivo expression of human T-lymphotropic Virus Type 1 Basic leucine-Zipper protein generates specific CD8+ and CD4+ T-lymphocyte responses that correlate with clinical outcome. J Infect Dis.;203:529-536 (2011).

Hivin P, Arpin-André C, Clerc I, Barbeau B and Mesnard J M. A modified version of a Fos-associated cluster in HBZ affects Jun transcriptional potency. Nucleic Acids Res. 34, 2761–2772.doi: 10.1093/nar/gkl375 (2006).

Hivin P, Basbous J, Raymond F, Henaff D, Arpin-Andre C, Robert- Hebmann V. The HBZ-SP1 isoform of human T-cell leukemia virus type I represses JunB activity by sequestration into nuclear bodies. Retrovirology 4, 14.doi: 10.1186/1742-4690-4-14 (2007).

Hivin P, Frédéric M, Arpin-André C, Basbous J, Gay B, Thébault S. Nuclear localization of HTLV-I bZIP factor (HBZ) is mediated by three distinct motifs. J. CellSci. 118, 1355–1362.doi: 10.1242/jcs.01727 (2005).

Horiuchi S, Yamamoto N, Dewan M Z, Takahashi Y, Yamashita A, Yoshida T, Nowell M, Richards P J, Jones SM, Yamamoto N. Human T-cell leukemia virus type-I Tax induces expression of interleukin-6 receptor (IL-6R): Shedding of soluble IL-6R and activation of STAT3 signaling. Int. J. Cancer: 119, 823–830 (2006).

Kannian P, Yin H, Doueiri R, Lairmore M D, Fernandez S, Green P L. Distinct transformation tropism exhibited by human T lymphotropic virus type 1 (HTLV-1) and HTLV-2 is the result of postinfection T cell clonal expansion. J. Virol. 86 3757–3766 10.1128/JVI.06900-11 (2012).

Karube K, Ohshima K, Tsuchiya T. Expression of FoxP3, a key molecule in CD4+CD25+ regulatory T cells, in adult T-cell leukaemia/lymphoma cells. British J Haematol.;126:81-84 (2004).

Kuhlmann AS, Villaudy J, Gazzolo L, Castellazzi M, Mesnard J M DucDodon M. HTLV-1 HBZ cooperates with JunD to enhance transcription of the human telomerase reverse transcriptase gene (hTERT). Retrovirology 4, 92.doi: 10.1186/1742-4690-4-92 (2007).

Landry S, Halin M, Vargas A, Lemasson I, Mesnard J M, Barbeau B. Upregulation of human T-cell leukemia virus type 1 antisense transcription by the viral tax protein. J. Virol., 83, 2048–2054 (2009).

Lemasson I, Lewis M R, Polakowski N, Hivin P, Cavanagh M H, Thebault S. Human T-cell leukemia virus type1 (HTLV-1) bZIP protein interacts with the cellular transcription factor CREB to inhibit HTLV-1transcription. J. Virol. 81, 1543–1553.doi:10.1128/JVI. 00480-06 (2007).

Ma G, Yasunaga J, Fan J, Yanagawa S, Matsuoka M. HTLV-1 bZIP factor dysregulates the Wnt pathways to support prolifer- ation and migration of adult T cell leukemia cells. Oncogene doi: 10.1038/onc.2012.450 (2012).

Macnamara A, Rowan A, Hilburn S, Kadolsky U, Fujiwara H, Suemori K. HLA class I binding of HBZ determines outcome in HTLV-1 infection. PLoS Pathog. 6:e1001117 10.1371/journal.ppat.1001117 (2010).

Maeda M, Shimizu A, Ikuta K, Okamoto H, Kashihara M, Uchiyama T, Honjo T, Yodoi J. Origin of human T-lymphotrophic virus I-positive T cell lines in adult T cell leukemia. Analysis of T cell receptor gene rearrangement. J Exp Med.;162(6):2169-74 (1985).

Manel N, Kim F J, Kinet S, Taylor N, Sitbon M, Battini J L. The ubiquitous glucose transporter GLUT-1 is a receptor for HTLV. Cell **115**(4):449–59 (2003).

Matsumoto J, Ohshima T, Isono O, Shimotohno K. HTLV-1 HBZ suppresses AP-1 activity by impairing both the DNA-binding ability and the stability of c-Jun protein. Oncogene 24, 1001–1010 (2005).

Matsuoka M and Jeang K T. Human T-cell leukaemia virus type1 (HTLV-1) infectivity and cellular transformation.Nat. Rev. Cancer7, 270-280 (2007).

Matsuoka M and Kuan-Teh J. Human T-cell leukaemia virus type 1 (HTLV-1) infectivity and cellular transformation, Nature Reviews Cancer 7, 270-280 (2007).

Matsuoka M and Yasunaga J I. Human T-cell leukemia virus type 1: replication, proliferation and propagation by Tax and HTLV-1 bZIP factor. Curr Op Virol.; 3:684-691 (2013).

Mochizuki M, Watanabe T, Yamaguchi K, Takatsuki K, Yoshimura K,Shirao M, Nakashima S, Mori S, Araki S, Miyata N. HTLV-I uveitis:a distinct clinical entity caused by HTLV-I.Jpn J Cancer Res, 83:236-239 (1992).

Nishioka K, Maruyama I, Sato K, Kitajima I, Nakajima Y, Osame M. Chronic inflammatory arthropathy associated with HTLV-I, Lancet, 1:441 (1989).

Pellegrini F P, Marinoni M, Frangione V. Down syndrome, autoimmunity and T regulatory cells. Clin Exp Immunol.169:238-243 (2012).

Poiesz B J, Ruscetti F W, Gazdar A F, Bunn P A, Minna J D, Gallo R C. Detection and isolation of type C retrovirus particles from fresh and cultured lymphocytes of a patient with cutaneous T-cell lymphoma. Proc Natl Acad Sci U S A. 77(12):7415-9 (1980).

Rende F, Cavallari I, Corradin A, Silic-Benussi M, Toulza F, Toffolo G M. Kinetics and intracellular compartmentalization of HTLV-1 gene expression:nuclear retention of HBZ mRNAs. Blood 117, 4855–4859. doi: 10.1182/blood- 2010-11-316463 (2011).

Satou Y, Yasunaga J, Yoshida M, Matsuoka M. HTLV-I basic leucine zipper factor gene mRNA supports proliferation of adult T cell leukemia cells. Proc. Natl. Acad. Sci. U. S. A. 103, 720–725 (2006).

Satou Y, Yasunaga J, Zhao T. HTLV-1 bZIP factor induces T-cell lymphoma and systemic inflammation in vivo. PLoS Pathogens. 7:e1001274 (2011).

Suemori K, Fujiwara H, Ochi T. HBZ is an immunogenic protein, but not a target antigen for human T-cell leukemia virus type 1-specific cytotoxic T lymphocytes. J Gen Virol. 90:1806-1811 (2009).

Sugata K, Satou Y, Yasunaga J, Hara H, Ohshima K, Utsunomiya A, Mitsuyama M, Matsuoka M. HTLV-1 bZIP factor impairs cell-mediated immunity by suppressing production of Th1 cytokines .Blood, 119(2):434-44 (2012).

Sugimoto M, Nakashima H, Watanabe S. T-lymphocyte alveolitis in HTLV-I-associated myelopathy. Lancet, 2(8569):1220 (1987).

Suzuki T, Uchida-Toita M, Yoshida M. Oncogene 18, 4137–4143 (1999).

T Usui, K Yanagihara, K Tsukasaki, K Murata1, H Hasegawa1, Y Yamada, S Kamihira. Characteristic expression of HTLV-1 basic zipper factor (HBZ) transcripts in HTLV-1 provirus-positive cells. Retrovirology; 10.1186/1742-4690-5-34 (2008).

Takatsuki K, Matsuoka M, Yamaguchi K. ATL and HTLV-I-related diseases, Adult T-Cell Leukemia. New York: Oxford University Press; p. 1-27 (1994).

Takatsuki K. Discovery of adult T-cell leukemia. Retrovirology; 2, 16 (2005).

Takeda S, Maeda M, Morikawa S, Taniguchi Y, Yasunaga J, Nosaka K, Tanaka Y, Matsuoka M. Genetic and epigenetic inactivation of TAX gene in adult T-cell leukemia cell. Int. J. Cancer:109,559–567 (2004).

Thébault S, Basbous J, Hivin P, Devaux C, Mesnard J M. HBZ interacts with JunD and stimulates its transcriptional activity. FEBS Lett., 562, 165–170 (2004).

Thébault S, Gachon F, Gaudray G, Mesnard J M. Regulation of human T-cell leukemia virus type I genome transcription by the viral Tax protein. Recent Res. Dev. Virol. 3**:**151-164 (2001).

Tosi G, Forlani G, Andresen V. Major Histocompatibility Complex Class II Transactivator CIITA is a viral restriction factor that targets human T-Cell Lymphotropic Virus type 1 Tax-1 function and inhibits viral replication. J Virol. 85:10719-10729 (2011).

Toulza F, Heaps A, Y T, Taylor GP, Bangham CR. High frequency of CD4+ FoxP3+ cells in HTLV-1 infection: inverse correlation with HTLV-1-specific CTL response. Blood; 111:5047-5053 (2008).

Van Dooren S, Salemi M, Vandamme AM. Dating the origin of the African human T-cell lymphotropic virus type-1 (HTLV-I) subtypes. Mol Biol Evol. Apr;18(4):661-71 (2001).

Verdonck K, González E, Van Dooren S, Vandamme A M, Vanham G, Gotuzzo E. Human T-lymphotropic virus 1: Recent knowledge about an ancient infection. The Lancet Infectious Diseases **7** (4): 266 (2007).

Yoshida M, Satou Y, Yasunaga J, Fujisawa J I, Matsuoka M. Transcriptional control of spliced and unspliced HTLV-1 bZIP factor gene. J. Virol., 82, 9359–9368 (2008).

Yoshida M. Multiple viral strategies of HTLV-1 for dysregulation of cell growth control**.** Annu. Rev. Immunol. 19**,** 475–496 (2001).

Zhao T, Satou Y, Sugata K, Miyazato P, Green P L, Imamura T. HTLV-1 bZIP factor enhances TGF-beta signaling through p300 coactivator. Blood 118, 1865–1876.doi:10.1182/blood- 2010-12-326199 (2011).

Zhao T, Yasunaga J, Satou Y, Nakao M, Takahashi M, Fujii M, Matsuoka M. Human T-cell leukemia virus type 1 bZIP factor selectively suppresses the classical pathway of NF-kappaB. Blood, 113, 2755–2764 (2009).